Universiteit
Leiden
The Netherlands

Toll-like receptor signaling in the innate immune system of zebrafish larvae

Yang, S.

Citation
Yang, S. (2016, December 20). *Toll-like receptor signaling in the innate immune system of zebrafish larvae*. Retrieved from https://hdl.handle.net/1887/45057

Version:	Not Applicable (or Unknown)
License:	Licence agreement concerning inclusion of doctoral thesis in the Institutional Repository of the University of Leiden
Downloaded from:	https://hdl.handle.net/1887/45057

Note: To cite this publication please use the final published version (if applicable).

Cover Page

Universiteit Leiden

The handle http://hdl.handle.net/1887/45057 holds various files of this Leiden University dissertation.

Author: Yang, S.
Title: Toll-like receptor signaling in the innate immune system of zebrafish larvae
Issue Date: 2016-12-20

CHAPTER 3

Tlr2 function in innate immune responses to *Mycobacterium marinum* infection in zebrafish

3

Shuxin Yang[1], Yasuhito Shimada[1,4], Zhan Xiong[2], Fons Verbeek[2], Rubén Marín-Juez[3], Annemarie H. Meijer[1], Herman P. Spaink[1*]

1 Institute of Biology, Leiden University, P.O. Box 9502, 2300 RA Leiden, the Netherlands 2 Leiden Institute of Advanced Computer Science, P.O. Box 9512, 2300 RA Leiden, the Netherlands 3 Department of Developmental Genetics, Max Planck Institute for Heart and Lung Research, Ludwigstrasse 43, 61231 Bad Nauheim, Germany 4 Department of Molecular and Cellular Pharmacology, Pharmacogenomics and Pharmacoinformatics, Mie University Graduate School of Medicine, Japan.

Abstract

TLR2 is known to play controversial roles in host defense against pathogens, especially *Mycobacterium tuberculosis* (Mtb). To study the function of TLR2 in mycobacterial infection, we analyzed a *tlr2* zebrafish mutant and infected larvae with *Mycobacterium marinum* (Mm), a close relative to Mtb, as a model for tuberculosis. After Mm infection, bacteria proliferated in *tlr2*$^{-/-}$ fish more than in the heterozygote *tlr2*$^{+/-}$, suggesting that Tlr2 is involved as a protective factor in host defense. We observed a reduced number of granulomas in *tlr2*$^{-/-}$ larvae when compared to the control. We also found that the *tlr2* mutant (*tlr2*$^{-/-}$) shows a reduced number of macrophages in the absence of infection. However, the macrophage migration speed and maximum migration distance from infection sites of phagocytic macrophages, are significantly higher in *tlr2*$^{-/-}$ than in *tlr2*$^{+/-}$ larvae. These results suggest that Tlr2 might be playing a role in macrophage congregation and phagocytosis. RNAseq analysis of infection experiments in mutant versus control showed that the number of upregulated and downregulated genes in the control was greatly diminished in the *tlr2* mutant, with the strongest effect on the down-regulated gene set. Detailed gene expression analysis using RNAseq and qPCR showed that Mm infection of *tlr2* mutant leads to decreased mRNA levels of genes involved in inflammation and immune responses, including *il1b*, *tnfb*, *cxcl11aa/ac*, *fosl1a* and *cebpb*. Furthermore, RNAseq analysis revealed that genes for Maf family transcription factors (Mafb/c-Maf), vitamin D receptors (Vdr) and diverse immunoglobulin domain-containing proteins (Dicps) are significantly different regulated in *tlr2* mutants with or without infection. This could result from a function in the control of induction of cytokines and chemokines as well as macrophage number, migration and phagocytosis. Moreover, our transcriptome analysis revealed Tlr2-specific pathways involved in Mm infection, which are also related to responses to Mtb infection in human macrophages. The expression analyses give further support for a function of TLR2 in host defense.

Introduction

Mycobacterium tuberculosis (Mtb) is the causative agent of tuberculosis (TB), which infects nearly one-third of the world's population, and kills about 1.5 million people annually (WHO Global Tuberculosis Report 2015). TB is characterized by the formation of granulomas not only in the lung but also in other tissues and organs. This is the result of a concerted action of host innate and adaptive immunity (1, 2).

Innate immune responses play a critical role in defense against TB infection in the host, and for a major part these processes are mediated by Toll-like receptors (TLRs), a conserved family of pattern recognition receptors. TLR2 is one of the most widely reported members of the TLRs family to be involved in defense against Mtb by virtue

of its recognition of cell wall-associated components associated with this pathogen (3-6). Following mycobacterial infection in human cell cultures, TLR2 dimerizes with TLR1 or TLR6, and recognizes mycobacterial components such as cell wall glycolipids LAM and LM (7), 38-kDa and 19kD mycobacterial glycoprotein (LpqH) (8-10), phosphatidylinositol mannoside (PIM) (11), and triacylated (TLR2/TLR1) (12, 13) or diacylated (TLR2/TLR6) lipoproteins (14, 15). Then these heterodimers recruit the Myd88 and Tirap (Mal) proteins to activate the IRAK(1 and 4)/TRAF6/IKK(α or β) cascade, which subsequently leads to the ubiquitination of IκBα and the activation of transcription factor NF-κB or AP-1 to release cytokines and chemokines (16, 17). Finally, these cytokines and chemokines attract migration of macrophages and neutrophils to the infection site leading to phagocytosis of bacteria. Tlr2 is shown to be a factor that is needed for granuloma formation in Mtb infection (18). Some studies have reported that $Tlr2^{-/-}$ mice lose control to high dose infection of Mtb or show higher susceptibility to Mtb infection compared to the wildtype (19, 20). Tlr2 also mediates the inhibition of MHC-II expression on the macrophage surface and MHC-II antigen processing by Mtb bacilli, thereby preventing presentation of Mtb antigens and decrease recognition by $CD4^+$ T cells, which may allow intracellular Mtb to evade immune surveillance and maintain chronic infection (10, 21). The interaction between TLR2 and Mtb or other pathogens not only promotes the killing of bacteria, but also seems to be a part of the bacterium's strategy to evade the immune system (22-24). For instance, LprG from Mtb was reported to inhibit human macrophage class II MHC antigen processing through TLR signaling (22). Furthermore, Tlr2 mutants of mice have an increased resistance against infection of *Candida albicans* (25) and *Yersinia pestis* (26). It has been proposed that this is the result of Tlr2-dependent induction of the anti-inflammatory cytokine IL-10 (26). Furthermore, TLR2 activation inhibits the release of IL-12 via activation of the cFos transcription factor. It also has been shown that IFN-γ or IFN-γ-induced signals (27) are inhibited after infection of murine macrophages in a Tlr2-dependent fashion (28). These effects show that TLR2 activation can yield a bias to T helper Type 2 (Th2) cells (29), and by breaking the Th1/Th2 balance can lead to less Th1 type responses and reducing the killing of intracellular pathogens. However, most of the molecular mechanisms underlying TLR2 functions remain unknown and a better understanding of the TLR2-mediated immune response and immune evasion can help in planning prevention and therapy strategies against Mtb infection.

Animal models have shown their power in studies of the mechanisms of interaction of host and TB pathogens, and discovering new anti-TB drugs. Zebrafish –adult and larvae– models have become a prevailing complement for rodent studies, for three important reasons. First, zebrafish have a 3-4 weeks separation stage between development of innate and adaptive immunity after fertilization (30, 31), which gives the possibility to study the host innate immune response to infection in the absence of

adaptive immune responses. Second, zebrafish can be infected by *Mycobacterium marinum* (Mm), a natural pathogen of cold blooded vertebrates and a close relative of Mtb, which can induce granuloma formation in zebrafish, and this is similar to human TB symptoms (32, 33). Third, the transparent larvae are ideal for imaging the early steps of the infection process in real time. Hence, zebrafish has earned its place of being a versatile tuberculosis model (34). In our previous study, we demonstrated that the mammalian TLR2 ligand Pam3CSK4, a synthetic triacylated lipopeptide that mimics the triacylated lipoprotein of mycobacteria, could also specifically activate the zebrafish Tlr2 pathway, inducing *fosl1a* and *cebpb* gene upregulation (35).

In the current study, to further explore the involvement of Tlr2 in Mm infection, we conducted infection studies using *tlr2* mutant zebrafish. We found that *tlr2* mutation promoted Mm infection, affected macrophage functions and corresponded with reduced granuloma formation compared to the wildtype. In summary, we demonstrated that Tlr2 plays an important role in protecting the host during the early stage of mycobacterial infection. In addition, we performed RNA deep sequencing (RNAseq) and determined a Tlr2-specific gene list for the response to Mm infection. In particular, this revealed that most of the downregulation of genes caused by Mm infection in the control was abrogated by *tlr2* mutation.

Results

1 tlr2 mutation prevents activation of tlr2-dependent genes in zebrafish larvae

The *tlr2*^{sa19423} mutant (*tlr2*$^{-/-}$) carries a thymine to adenine point mutation that creates a premature stop codon (Fig. 1A), which is located in the C-terminus of the leucine-rich repeat (LRR) domain. This leads to a truncated protein without the Toll/IL-1 receptor (TIR) domain, which is required for the interaction with Myd88 and Tirap (Mal) (36, 37).

To confirm whether *tlr2* mutation blocks its downstream pathway, we analyzed the gene expression profiles of zebrafish treated with the TLR2 agonist, Pam3CSK4. Pam3CSK4 was injected into the blood island of zebrafish embryos at 27 hpf. One hour after injection (hpi), we collected samples and performed qPCR to analyze the expression levels of TLR2-downstream effectors, CCAAT/enhancer-binding protein beta *(cebpb*) and FOS Like Antigen 1a (*fosl1a*), as we previously reported to be specific targets of Tlr2 signaling (35). In *tlr2*$^{+/\ sa19423}$ heterozygotes (*tlr2*$^{+/-}$), the expressional levels of transcription factors *cebpb* and *fosl1a*, and inflammation marker gene *il1b* were significantly induced by Pam3CSK4, whereas *tlr2*$^{-/-}$ showed no significant response (Fig. 1B). To confirm that these results are specific for the TLR2 pathway, we injected flagellin, a TLR5 agonist into 27 hpf embryos. Flagellin induced the non-specific

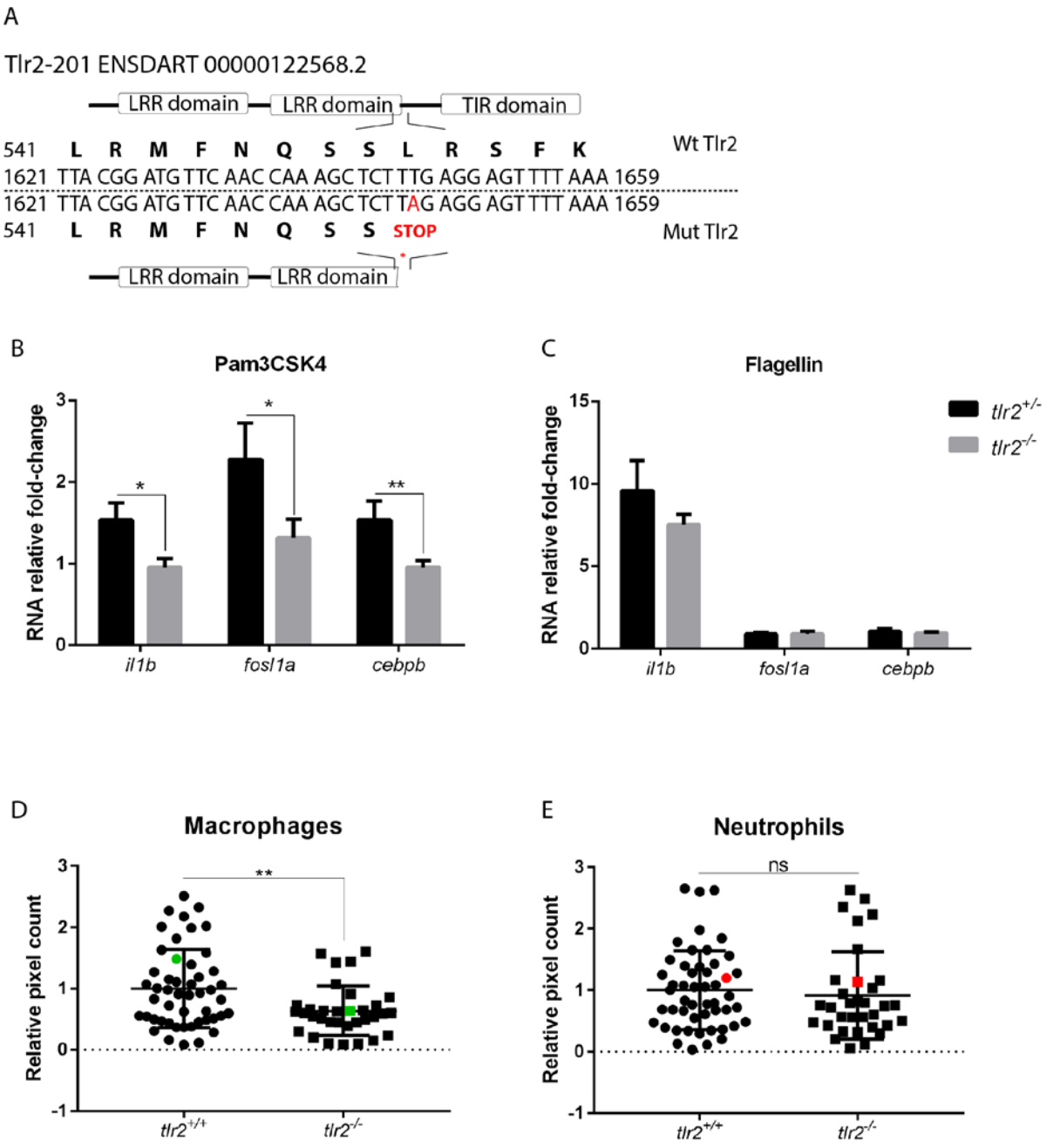

FIGURE 1 Characterization of the Tlr2 mutant. A, mutant DNA and protein sequence. A point mutation (T to A) in the C-terminal of the second LRR domain of zebrafish Tlr2 introduces a premature stop codon. The predicted truncated protein lacks the whole TIR domain. Nucleotide and amino acid positions are indicated with respect to the translation start codon. B and C, *tlr2*$^{-/-}$ and *tlr2*$^{+/-}$ embryos were injected at 27 hpf with 1 ng Pam3CSK4 or 0.1ng flagellin and expression levels of *il1b*, *fosl1a* and *cebpb* were determined at 1 hour post injection by qPCR. Data (mean ± SEM) are combined from at least three biological replicates (n=10 embryos per group) and expressed relative to their corresponding mock injection (water) control, which is set at 1. Statistical significance of differences between mock and Pam3CSK4 groups was determined by two-way ANOVA with Sidak Multiple Comparison test as a post-hoc test, *p < 0.05, **p<0,01. D, fluorescence relative pixel-count

analyses of GFP-labeled macrophages in 2dpf *tlr2*$^{+/+}$/*Tg*(*mpeg1*:*EGFP*) and *tlr2*$^{-/-}$/*Tg*(*mpeg1*:*EGFP*) embryos (at least 35 embryos per group) were performed based on stereo fluorescence images (green symbols indicate the data point for which representative examples are shown in figure S4). E, fluorescence relative pixel-count values of neutrophils derived from images of whole mount TSA immune staining (red symbols indicate the data point for which representative examples are shown in figure S4). Data (mean ± SD) are combined from two individual experiments. Statistical significance of differences was determined by T-test, **p<0.01, ns, no significant difference.

inflammation marker *il1b* expression, but not *cebpb* and *fosl1a* expression in both *tlr2*$^{+/-}$ and *tlr2*$^{-/-}$ larvae (Fig. 1C). Overall, these data show that *tlr2* mutation specifically blocks its downstream pathways.

2 Macrophage and neutrophil phenotype in tlr2 mutant

To study the effects of *tlr2* mutation in immune cells, we conducted two individual experiments of TSA staining with 2dpf *tlr2*$^{+/+/}$*Tg*(*mpeg1:EGFP*) and *tlr2*$^{-/-}$*Tg*(*mpeg1:EGFP*) larvae. TSA staining detects Mpx activity, which is specific for neutrophils in zebrafish embryos and larvae. The combination of using *mpeg1*-EGFP fish lines and TSA staining can be used to distinguish macrophages (*mpeg1:*EGFP-positive, TSA-negative) and neutrophils (*mpeg1:*EGFP-negative, TSA-positive) (38). The numbers of macrophages in *tlr2*$^{-/-}$ larvae were significantly reduced compared to those in *tlr2*$^{+/+}$ (Fig. 1D and Fig. S4) while the numbers of neutrophils was not significantly different between these groups (Fig. 1E and Fig. S4). We also conducted TSA staining in 2 dpf *tlr2*$^{+/-}$ and *tlr2*$^{-/-}$ larvae without the m*peg1:gfp* marker, and confirmed that there was no significant reduction of neutrophils induced by *tlr2* mutation Fig. S1). These results indicate that *tlr2* mutation does not affect the development of neutrophils but may influence macrophage development.

3 Mycobacterium marinum infection in tlr2 knockdown or mutant larvae

We injected 28 hpf *tlr2* morphants, standard control morphants, and *tlr2*$^{-/-}$ and *tlr2*$^{+/-}$ embryos with ~150 CFU Mma20 by blood island injection. The results of stereo fluorescence microscopy and pixel count analysis show that the bacterial burden in *tlr2* morphants was significantly higher than those of control larvae at 3 dpi (Fig. 2A). Considering the transient effect of morpholinos, we did not test later time points. In agreement, the bacterial burden was significantly higher in *tlr2*$^{-/-}$ than *tlr2*$^{+/-}$ larvae, with the most pronounced difference at 4dpi (Fig. 2B). Figure 2C represents the typical phenotype of infection in *tlr2*$^{+/-}$ and *tlr2*$^{-/-}$ larvae observed using confocal laser

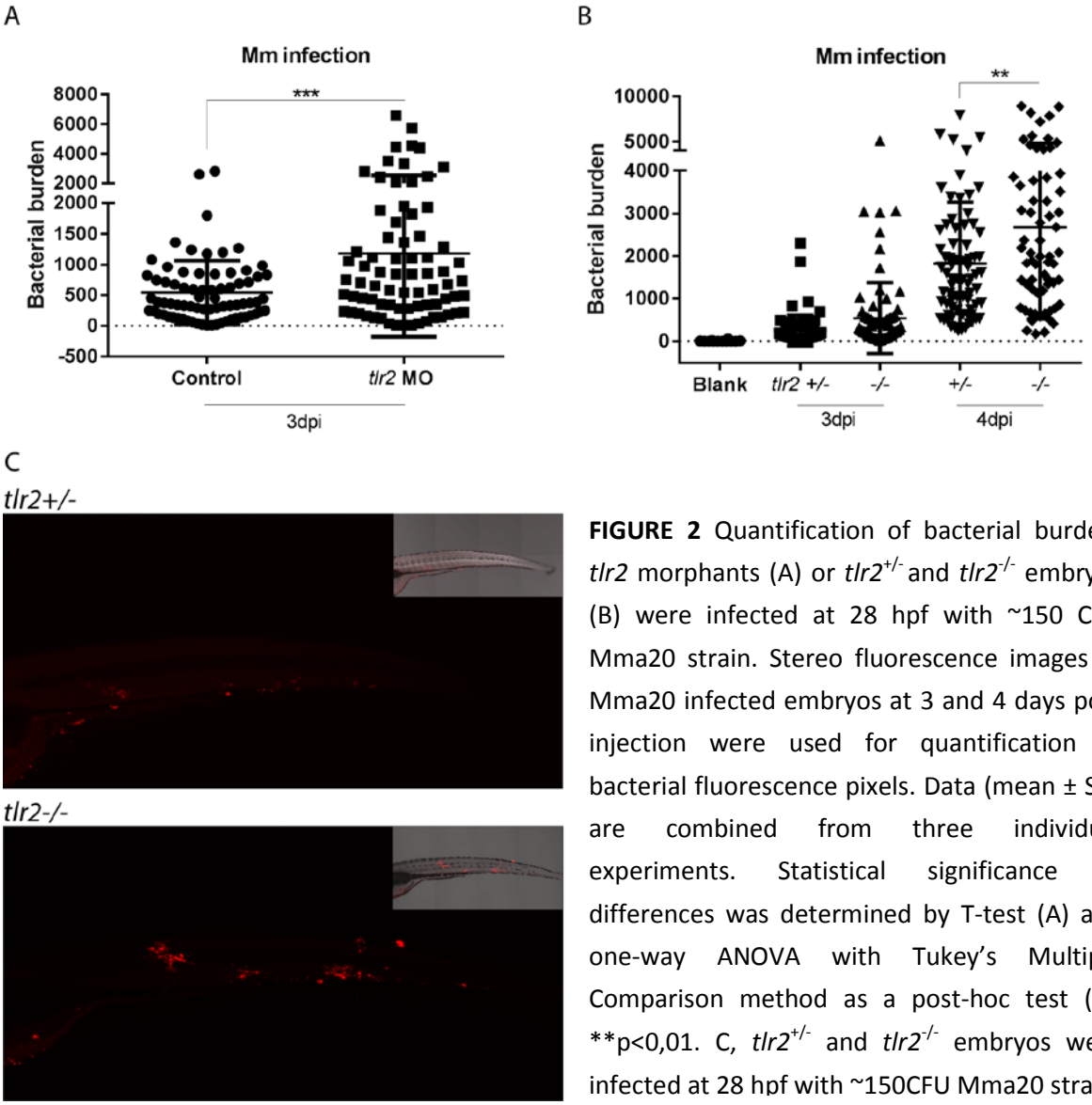

FIGURE 2 Quantification of bacterial burden. *tlr2* morphants (A) or *tlr2*$^{+/-}$ and *tlr2*$^{-/-}$ embryos (B) were infected at 28 hpf with ~150 CFU Mma20 strain. Stereo fluorescence images of Mma20 infected embryos at 3 and 4 days post injection were used for quantification of bacterial fluorescence pixels. Data (mean ± SD) are combined from three individual experiments. Statistical significance of differences was determined by T-test (A) and one-way ANOVA with Tukey's Multiple Comparison method as a post-hoc test (B). **p<0,01. C, *tlr2*$^{+/-}$ and *tlr2*$^{-/-}$ embryos were infected at 28 hpf with ~150CFU Mma20 strain.

scanning microscopy (CLSM) confirming that *tlr2* mutation promotes a higher bacterial burden during Mm infection.

Protective immunity and latent Mm infection in zebrafish are associated with the formation of mature protective granulomas (39). In mice studies, Tlr2-deficiency resulted in a defective granulomatous response (18, 20). To test whether *tlr2* mutation also suppresses the granuloma formation in zebrafish, we conducted CLSM imaging of *tlr2*$^{-/-}$*/Tg(mpeg1:EGFP)* and *tlr2*$^{+/+}$*/Tg(mpeg1:EGFP)* with Mma20 infection. We analyzed bacterial numbers and granuloma formation at several representative highly infected regions of zebrafish larvae at 4 dpi. We observed that *tlr2*$^{+/+}$ larvae showed normal granuloma formation and the majority of the bacteria was inside macrophages.(Fig. 3A-D). In contrast, in two representative locations in *tlr2*$^{-/-}$ larvae (Fig. 3E), a majority of the bacteria congested together and formed a big cluster without evidence for being

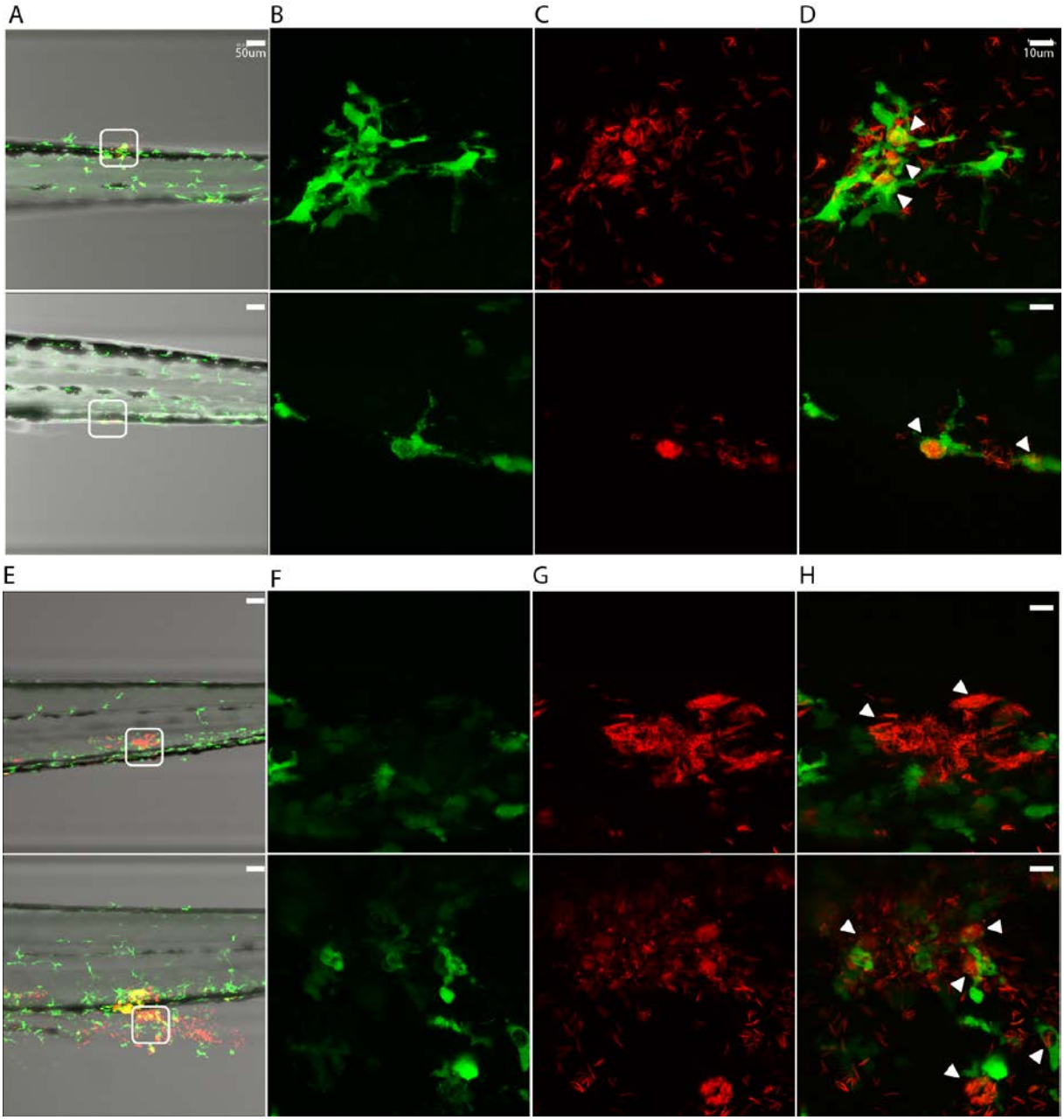

FIGURE 3 Granuloma formation and macrophage phenotypes in the Tlr2 mutant upon Mma20 infection. The *tlr2*$^{+/+}$/*Tg*(*mpeg1*:*EGFP*) (A-D) and *tlr2*$^{-/-}$/*Tg*(*mpeg1*:*EGFP*) (E-H) embryos were infected at 28 hpf with ~150CFU Mma20 strain. Confocal laser scanning imaging was conducted using a Leica SP1 microscope with 10 (A, E) and 63 (B-D and F-H) times magnification lenses. GFP-green, macrophage; mCherry-red, Mma20; white arrow head indicates the enlarged section of this picture. The size bar in bright view figure A represents 50um, in fluorescence view figure D represents 10um. (B-D and F-H) enlargements of the areas indicated in panels A and E. The positions indicated by arrowheads are the reference points. In the Tlr2 mutant they point to clusters of bacteria that are not present inside macrophages. In the control they point to macrophages that have ingested bacteria, which are observed much more frequently than in the mutant. The images are representative of images from 38 *tlr2* mutant and 42 wildtype embryos.

inside macrophages. (Fig. 3E-H). Furthermore, these results show that the *tlr2*$^{-/-}$ mutant allows higher Mm proliferation and is impaired in granuloma formation compared to the *tlr2*$^{+/+}$ control.

To further quantify the migration of macrophages after Mm infection, we performed cell tracking to measure the maximum migration distance from the start of the image sequence and their average speed from 84 to 96 hpi (Fig. 4). In this study, the location of the bacteria-containing macrophages in the first frame of the movie was set as the origin and we then tracked the migration of the macrophages during the following twelve hours. Our results show that both the maximum distance of migration and the average speed of macrophage migration in *tlr2*$^{-/-}$ was significantly higher than that in *tlr2*$^{+/+}$ (Fig. 4C and D). These results show that *tlr2* mutation affects macrophage migration after infection.

4 Tlr2-specific gene expression profiles after Mycobacterium marinum infection

To assess the general inflammation and specific immune responses in *tlr2* mutants, we studied mRNA expression levels of *il1b*, *tnfa*, *tnfb*, *irg1l* , and *tlr2* specific transcription factors *fosl1a* and *cebpb* in *tlr2*$^{-/-}$ and *tlr2*$^{+/-}$ larvae upon Mma20 infection by qPCR at 4dpi. Our results show that the expression levels of *il1b* and *tnf* in *tlr2*$^{-/-}$ larvae are significant reduced (Fig. 5A-C). The induction of *cebpb* and *fosl1a* was inhibited in *tlr2*$^{-/-}$ larvae (Fig. 5E, F). The expression of *irg1l* showed no significant difference between infection and non-infection in the *tlr2*$^{-/-}$ larvae (Fig. 5D). In previous work from our laboratory, Cxcl11-like chemokines were shown to play a crucial role in macrophage-mediated granuloma formation upon Mm infection (40). We therefore conducted qPCR to characterize the expression level of *cxcl11-like* genes, previously shown to be infection inducible (40), including *cxcl11aa* and *cxcl11ac* (Fig.5G and H). The expression level of gene *cxcl11aa* and *cxcl11ac* was significantly higher in *tlr2*$^{+/-}$ larvae than in *tlr2*$^{-/-}$ upon Mm infection (Fig. 5G, H). These results indicate that *tlr2* mutation results in a defective immune or inflammatory response to Mm infection.

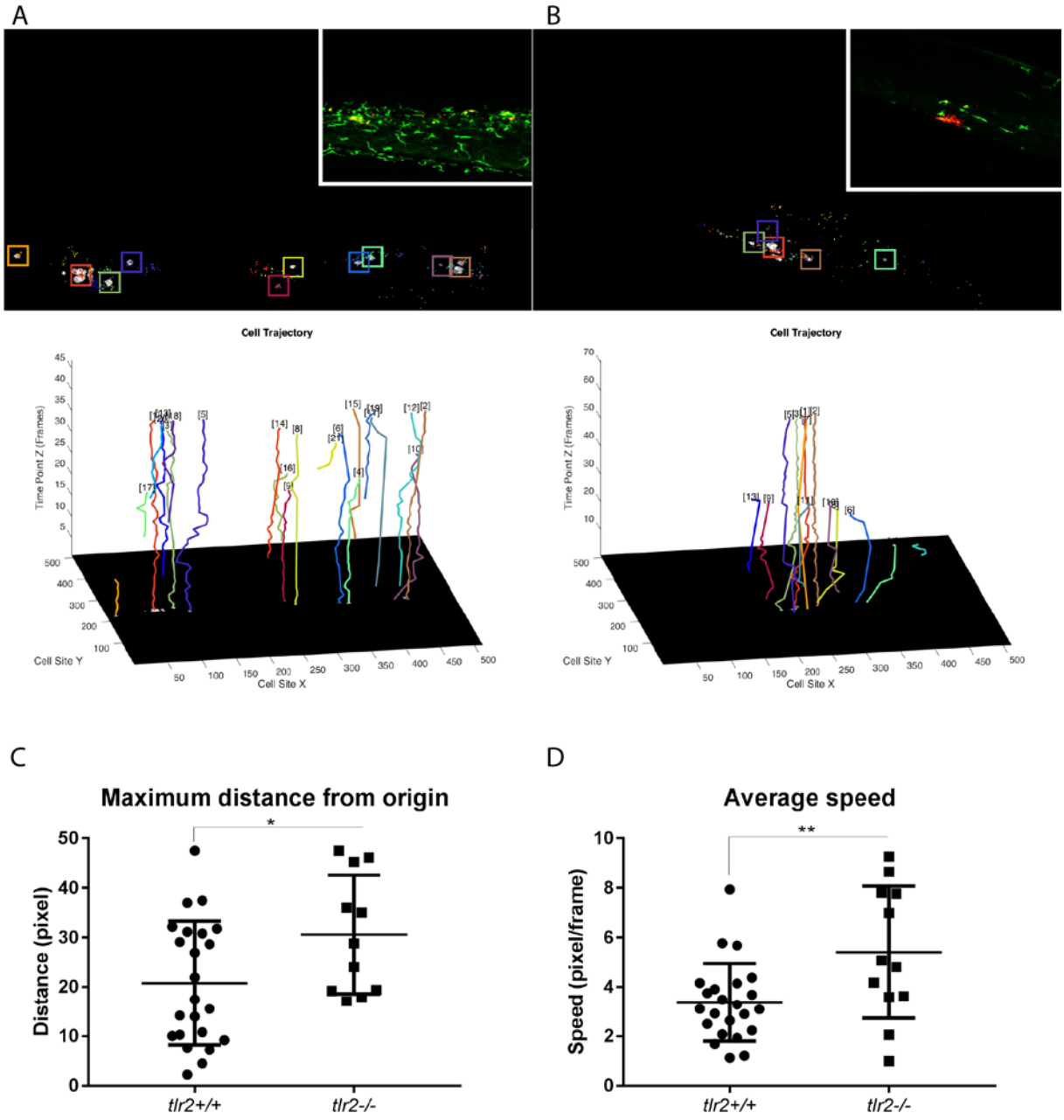

FIGURE 4 Cell tracking of macrophages in (A) *tlr2*$^{+/+}$/Tg(mpeg1:EGFP) and *tlr2*$^{-/-}$/Tg(mpeg1: EGFP) (B) larvae with Mm infection. Embryos were infected with ~150 CFU Mma20 strain at 28hpf, imaging was performed using a Nikon Eclipse Ti-E inverted microscope (40×) from 84hpi to 96hpi. There are 46 frames from *tlr2*$^{+/+}$ (A, bottom panel) and 70 from *tlr2*$^{-/-}$ (B, bottom-panel) that were analyzed, resulting in the reconstruction of 23 macrophage tracks in the wildtype and 12 in the mutant. The upper-panel in A and B shows the track of macrophages in 2D view, the insets are the original representative images and the bottom-panel shows that in 3D view. C and D, the maximum migration distance from the original site of infection in the first frame of the movie and the average speed of macrophages after phagocytosis of bacteria. The statistical significance of differences was determined by T-test. **p<0.01.

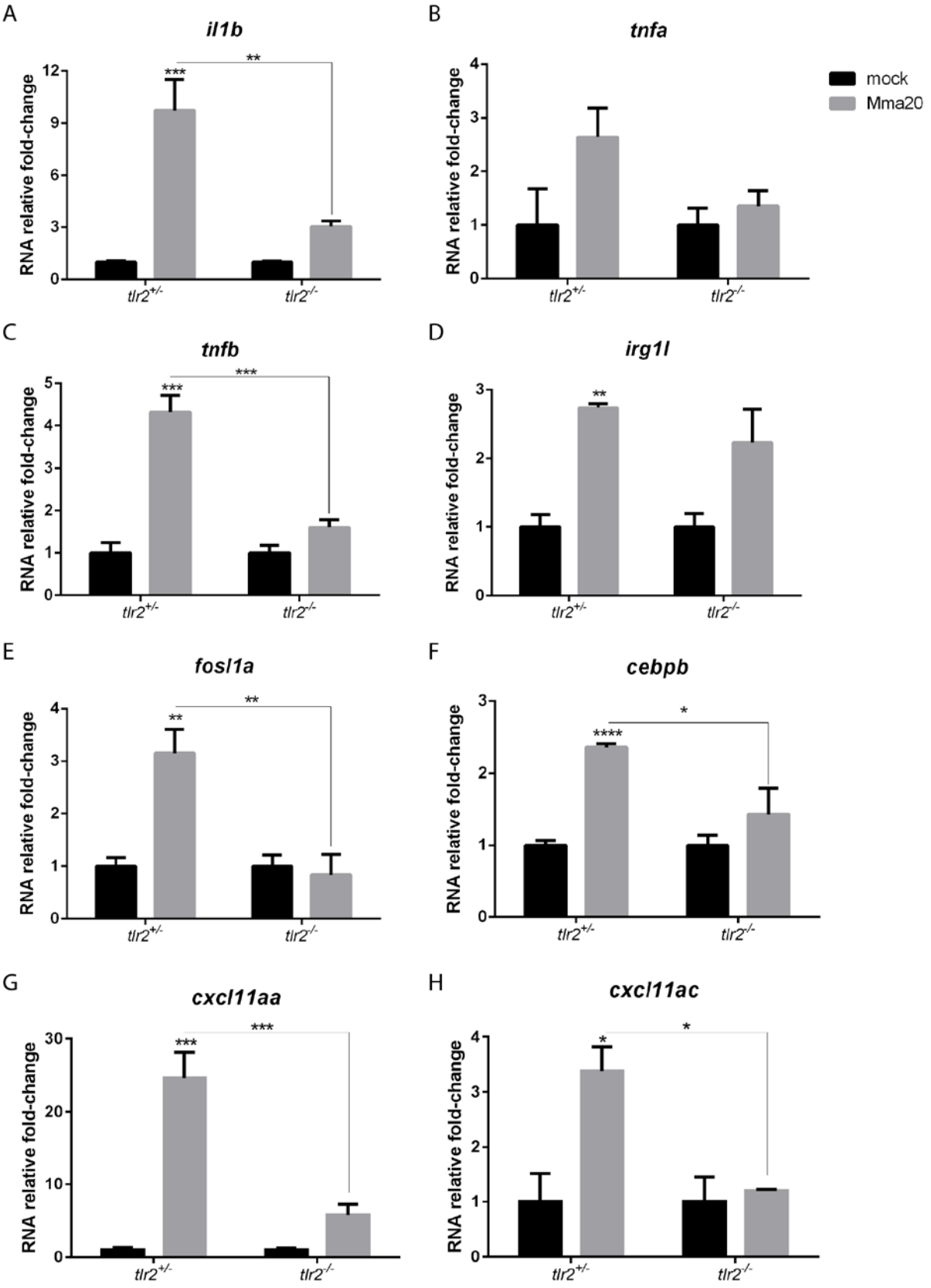

FIGURE 5 Immune genes expression in *tlr2*$^{+/-}$ and *tlr2*$^{-/-}$ fish lines infected with Mm. The expression levels of *il1b* (A), *tnfa* (B), *tnfb* (C), *irg1l* (D), *fosl1a* (E), *cebpb* (F), *cxcl11aa* (G) and *cxcl11ac* (H) were determined at 4dpi by qPCR. Data (mean ± SEM) are derived from at least three biological replicates

(n = 10 embryos per group) and expressed relative to their corresponding mock injection (PBS) control, which is set at 1. Statistical significance of differences was determined by two-way ANOVA with Sidak Multiple Comparison test as a post-hoc test. *p<0.05, **p<0.01, ****p<0.0001

To further study the function of *tlr2* in defense against mycobacterial infection, we performed RNAseq of *tlr2*$^{+/-}$ and *tlr2*$^{-/-}$ larvae infected with 150 CFU Mma20 at 4dpi and PBS-injected controls. We summarized the number of differentially expressed genes (DEGs) according to *p*-value (Fig. 6A, B). *tlr2*$^{+/-}$ induced an increased number of DEGs than *tlr2*$^{-/-}$ with Mma20 infection at any given *p*-value or false discovery rate less than 0.05, or any given fold-change with a *p*-value less than 0.05. The data also shows that most of the downregulation of genes caused by Mm infection in the control was abrogated by *tlr2* mutation (Fig. 6A, B). To further analyze these RNAseq data, we chose the genes with a threshold of a *p*-value less than 0.05 in *tlr2*$^{+/-}$ with Mma20 infection (1102 up- and 827 down-regulated genes, Fig. 6A). Then, for these 1102 and 827 genes, we calculated the ratio of the fold-change of *tlr2*$^{+/-}$ versus *tlr2*$^{-/-}$, after that, the genes with ratio greater than 2 or less than 0.5 were screened (Fig. 6C). As a result, 97 and 92 genes were selected as *tlr2* specific up- and down-regulated genes, respectively. We conducted gene ontology (GO) analysis (Fig. 6D, E) showing that genes that grouped into the immune system category are the most prominently deregulated (36%) in the whole *tlr2* up-regulated 97-gene set (Fig. 6D). Within this category we found genes involved in lysosome, chemotaxis, transcription regulation, diverse immunoglobulin domain-containing proteins (*dicps*) and other immune processes (Fig. 6D and 7A-E). For other process related categories, many up-regulated genes fell in the categories oxidation-reduction process, DNA repair, transcription regulation and apoptotic process regulation (Fig. S2). In the *tlr2* down-regulated 92-gene set, the immune related genes also were the largest portion (15%; Fig. 6E, 7F). The categories of non-immune related genes are listed in Fig. S3. Our results show that *tlr2* mutation leads to far less immune response genes that are upregulated upon Mm infection in zebrafish larvae.

To show the relationship between the genes that are differentially expressed, we constructed networks based on common expression targets in the 97 up- and 92 down-regulated genes (41). The involved networks with the up-regulated genes contain LIPC, NR0B2, HMGCR, ITLN1, FGF23, VDR, IRAK3 and TLR8 (Fig. S5). In the *tlr2*$^{+/-}$ control we observed positively regulated HMGCR, FGF23, VDR and TLR8, and negatively regulated NR0B2, whereas *tlr2*$^{-/-}$ shows an opposite regulation for most of them. However, LIPC and IRAK3, were positively regulated in both *tlr2*$^{+/-}$ and *tlr2*$^{-/-}$. For the 92 downregulated genes, a network containing NROB2 and MAFB was constructed (Fig. S6). NR0B2 and MAFB were positively regulated in *tlr2*$^{-/-}$ zebrafish and down regulated in *tlr2*$^{+/-}$.

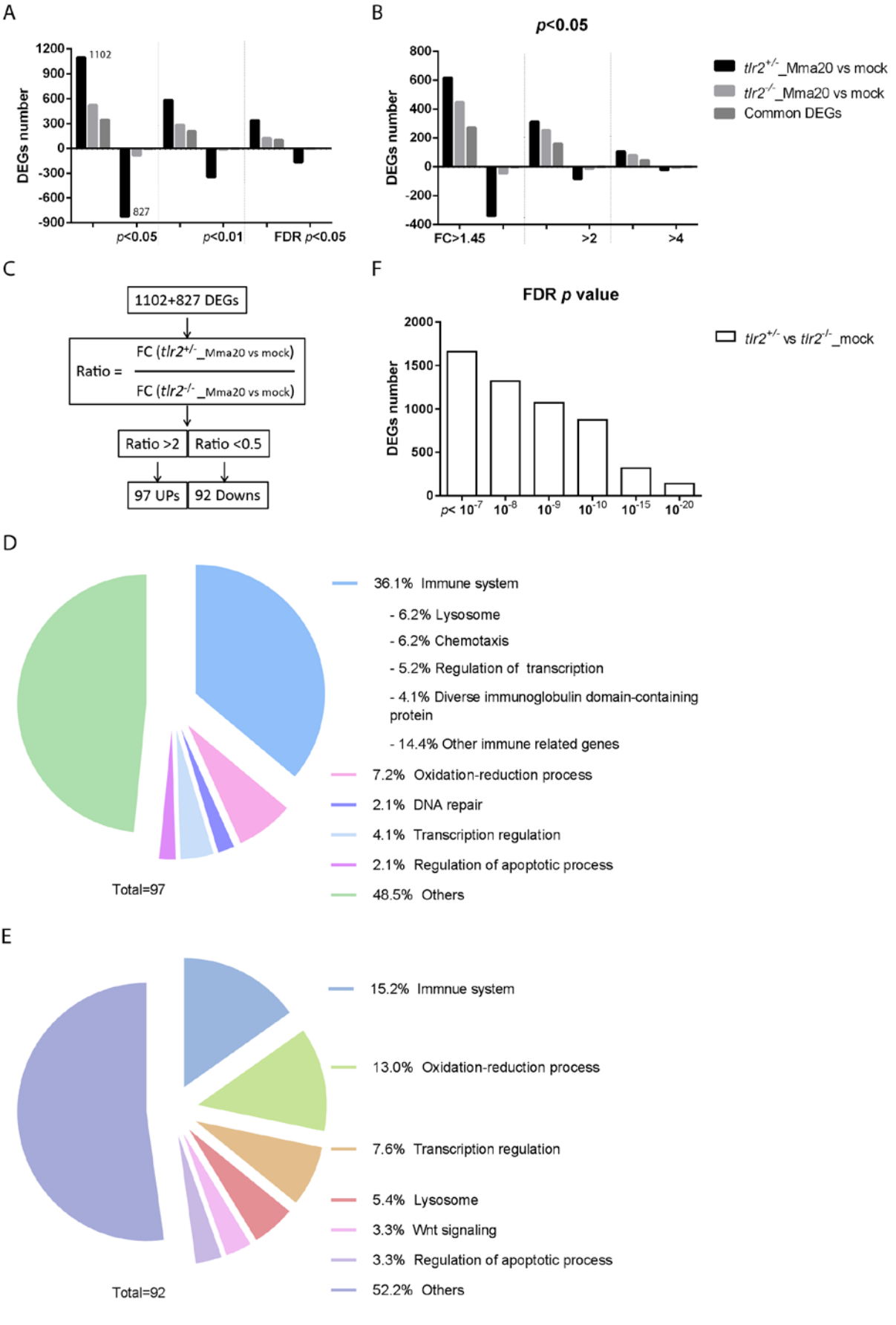
A
1200
900
600
300
0
-300
-600
-900
DEGs number
1102
827
p<0.05
p<0.01
FDR p<0.05
B
p<0.05
800
600
400
200
0
-200
-400
DEGs number
FC>1.45
>2
>4
tlr2+/-_Mma20 vs mock
tlr2-/-_Mma20 vs mock
Common DEGs
C
1102+827 DEGs
Ratio = FC (tlr2+/-_Mma20 vs mock) / FC (tlr2-/-_Mma20 vs mock)
Ratio >2
Ratio <0.5
97 UPs
92 Downs
F
FDR p value
2000
1500
1000
500
0
DEGs number
p< 10-7
10-8
10-9
10-10
10-15
10-20
tlr2+/- vs tlr2-/-_mock
D
36.1% Immune system
- 6.2% Lysosome
- 6.2% Chemotaxis
- 5.2% Regulation of transcription
- 4.1% Diverse immunoglobulin domain-containing protein
- 14.4% Other immune related genes
7.2% Oxidation-reduction process
2.1% DNA repair
4.1% Transcription regulation
2.1% Regulation of apoptotic process
48.5% Others
Total=97
E
15.2% Immnue system
13.0% Oxidation-reduction process
7.6% Transcription regulation
5.4% Lysosome
3.3% Wnt signaling
3.3% Regulation of apoptotic process
52.2% Others
Total=92

FIGURE 6 Overview of RNAseq results. A, B the number of DEGs of *tlr2*$^{+/-}$ and *tlr2*$^{-/-}$ strains infected with Mm compared to the control at different p-value and fold change. C, the work flow of screening genes of which the regulation by infection is dependent on *tlr2*. D, GO analysis of the 97 upregulated genes. E, GO analysis of the 92 down-regulated genes. FC, fold-change. F, the DEGs number of *tlr2*$^{-/-}$ versus *tlr2*$^{+/-}$ at different FDR p-value in the uninfected mock-injected condition.

5 Enrichment analysis of Tlr2 specific genes after Mycobacterium marinum infection

To link our data to gene sets defined based on prior biological knowledge (including GO), we conducted Gene-Set Enrichment Analysis (GSEA) of the genes of which the ratios of Mm infection and control in *tlr2*$^{+/-}$ or *tlr2*$^{-/-}$ zebrafish are significantly different without considering fold-changes. This method derives its power by focusing on gene sets, that is, groups of genes that share common biological function, chromosomal location, or regulation (42). Because the numbers of predicted gene sets were too large for our analysis method (more than 1,000 with $p < 0.05$), we focused on the gene sets related to metabolic, immunological and inflammation pathways. The GSEA predicted 61 pathways in *tlr2*$^{+/-}$ and 67 pathways in *tlr2*$^{-/-}$ zebrafish responsive to Mma20 infection (Supplementary Table 2A and 2B). Interestingly, most of these pathways are common in *tlr2*$^{+/-}$ and *tlr2*$^{-/-}$, however some of them are detected as being anti-correlated in regulation, including some pathways underlying natural killer cell functions and omega-6-fatty acid metabolism (Supplementary Table 2C). We also performed Sub-Network Enrichment Analysis (SNEA) (43) to identify possible key genes that are responsible for the difference in response of the *tlr2*+/- and *tlr2*-/- group to Mm infection ($p < 0.05$). SNEA predicted 565 and 503 pathways for *tlr2*$^{+/-}$ and *tlr2*$^{-/-}$ zebrafish that are linked to the response to infection, respectively (Supplementary Table 2D and 2E), and 264 and 202 of them are specific for the response in *tlr2*$^{+/-}$ and *tlr2*$^{-/-}$ fish, respectively (Supplementary Table 2F). Since the RNAseq was conducted with the total RNA from whole body of zebrafish, it is not possible to define which pathways are involved in macrophage functions related to *tlr2* expression. Therefore, we downloaded DNA microarray data (GDS4781) of human macrophages transfected with *M.tuberculosis* from Gene Expression Omnibus (44). SNEA analysis of human macrophages shows that 659 pathways are linked to Mtb infection (Supplementary Table 2G). By comparing human SNEA result to *tlr2*$^{+/-}$ specific pathways in zebrafish, 56 pathways were defined as *tlr2*$^{+/-}$-specific (Supplementary Table 2H). Of these, the pathway of TLR8, which has the lowest *p*-value in both zebrafish and human enrichment, and its network is depicted as example in Figure S7. In general these analysis show that the *tlr2*-/- mutant has a very different immune response of which many pathways that are linked to human tuberculosis are differently responding.

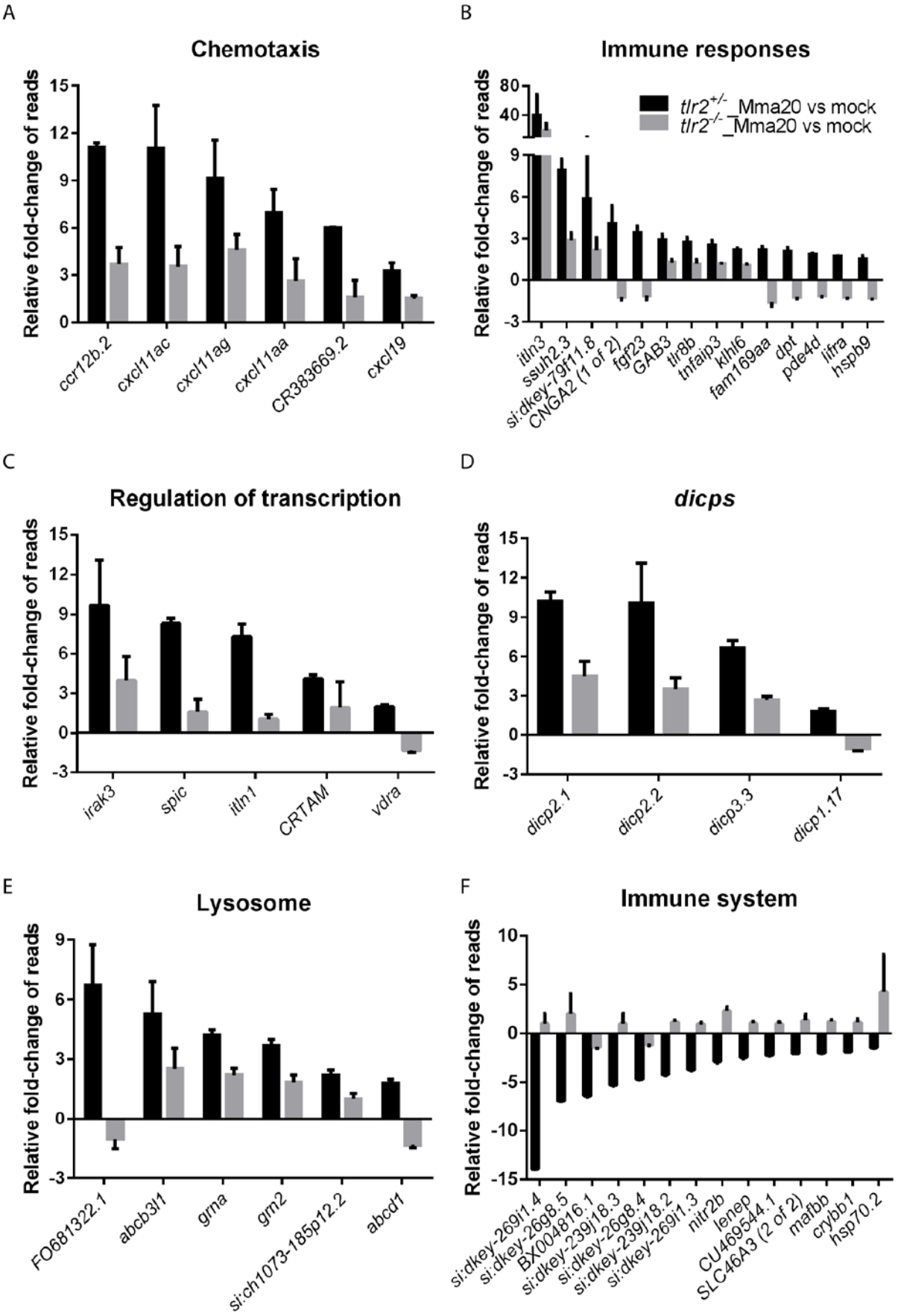
A
Chemotaxis
Relative fold-change of reads
15
12
9
6
3
0
ccr12b.2
cxcl11ac
cxcl11ag
cxcl11aa
CR383669.2
cxcl19
B
Immune responses
Relative fold-change of reads
80
40
9
6
3
0
-3
tlr2+/-_Mma20 vs mock
tlr2-/-_Mma20 vs mock
itln3
ssuh2.3
si:dkey-79f11.8
CNGA2 (1 of 2)
fgf23
GAB3
tlr8b
tnfaip3
klhl6
fam169aa
dpt
pde4d
lifra
hspb9
C
Regulation of transcription
Relative fold-change of reads
15
12
9
6
3
0
-3
irak3
spic
itln1
CRTAM
vdra
D
dicps
Relative fold-change of reads
15
12
9
6
3
0
-3
dicp2.1
dicp2.2
dicp3.3
dicp1.17
E
Lysosome
Relative fold-change of reads
9
6
3
0
-3
FO681322.1
abcb3l1
grna
gm2
si:ch1073-185p12.2
abcd1
F
Immune system
Relative fold-change of reads
10
5
0
-5
-10
-15
si:dkey-269i1.4
si:dkey-26g8.5
BX004816.1
si:dkey-239j18.3
si:dkey-26g8.4
si:dkey-239j18.2
si:dkey-269i1.3
nitr2b
lenep
CU469544.1
SLC46A3 (2 of 2)
mafbb
crybb1
hsp70.2

FIGURE 7 Overview of fold changes of representative genes selected from the gene categories resulting from GO-term analysis. A-E: *tlr2*-dependent genes with upregulation corresponding to Fig. 6D. F: *tlr2* specific genes with downregulation corresponding to Fig. 6E.

6 Comparison of gene expression profiles of tlr2 homozygote mutant with heterozygote

We compared basal levels of gene expression in the absence of infection between *tlr2* homozygote and heterozygote mutants. These results show that there is a large group of genes that are expressed differently even at extremely stringent *p*-values (Fig. 6F). To get possible indications whether the basal expression level differences of genes might be relevant to the Tlr2 pathway we performed GO analysis of a set of genes that were expressed differently with the very low FDR *p*-value of 10^{-10} (Supplementary Table 3). Our results show that there is a large enrichment of genes belonging to the GO terms related to neural development. In addition, we have also analyzed differences with a fold change criterion of two and FDR *p*-value of 0.05 (Supplementary Table 4). These analyses indicated that under the GO category transcription factor genes only two categories of genes including the c-Maf transcription factor (Supplementary Table 4) were present. Finally, the RNAseq analysis showed that the *mpeg1.1* gene is expressed approximately 2 fold higher in the $tlr2^{+/-}$ control than in the $tlr2^{-/-}$ mutant (Supplementary Table 5), consistent with the observation of reduced macrophage numbers in the *tlr2* mutant (Fig. 1D, Fig. S4).

Discussion

Our study created a systemic *tlr2* deficiency-Mm infection model in zebrafish larvae to study Tlr2 function in the innate immune system during mycobacterial infection. In alternative model systems for human tuberculosis that use mice, it is difficult to perform systemic studies at the genomic and microscopic level. As a result all the studies performed in mice have been carried out with isolated tissues. Furthermore, there are only a few RNA sequencing results of TB studies in rodents (45, 46), human serum (47), human pulmonary epithelial cells (48), and bovine systems (49-52). In zebrafish larvae it is possible to combine the advantage of studying the entire system using transcriptomics and zooming in on mechanisms of the infection process using fluorescence microscopy. Furthermore, as in rodents, the zebrafish offers excellent genetics tools for obtaining mutants such as the *tlr2* mutant described in this study. The deep sequencing data provided the chance to study the whole transcriptome profile in our mycobacterial infection model and revealed the panorama of *tlr2* signaling-related gene expression. Importantly, taking advantage of this model we

were able to document in vivo the impact that lack of Tlr2 has in the interaction between infecting bacteria and macrophages.

We have shown in this study that *tlr2* mutant leads to increased mycobacterial infection in zebrafish larvae. This result is similar to results from studies in Tlr2 knockout mice, where infection with Mtb resulted in increased lung infection and highly increased mortality (19, 20). However, in these works a role of Tlr2 could only be shown at high doses of infection, whereas at a low dose no effect was observed of the mutation (19,20). In the study of Drennan et al (20) it was shown that infection of the Tlr2 mutant leads to a decrease of the number of granulomas formed in the lungs. This is in line with our results where we found that the clustering of macrophages in pre-granuloma structures was strongly decreased. In addition, the study in mice showed that in the Tlr2 mutant there was an increased T cell response that was ineffective in combating progression of infection. Since in our larval system there is no adaptive response present, we can therefore not address this point and need to perform studies in adults in future studies. However, it is important that we can conclude that the role of Tlr2 in granuloma formation is not dependent on T cell activity. Furthermore, we can now also conclude that the function of Tlr2 in granuloma formation is at the very early steps of the infection process. We also observed that Tlr2 mutants in zebrafish larvae result in a decreased number of macrophages even in the absence of infection and this might attributed to the emergence and differentiation of hematopoietic stem and progenitor cells. He et al. (53) demonstrated that Tlr signaling-dependent inflammatory signaling is necessary and sufficient for hematopoietic stem and progenitor cells emergence in zebrafish, in the absence of infection or pathological inflammation. TLR2 agonist Pam3CSK4 was also shown to induce a large proportion of hematopoietic stem cells to express markers of the myelomonocytic lineage (54). On the other hand, Herman et al. (55) showed that systemic exposure of mice to a TLR2 agonist leads to an expansion of bone marrow and spleen phenotypic hematopoietic stem cells and progenitors, but a loss of hematopoietic stem cell self-renewal capacity. We also observed that the Tlr2 mutation in zebrafish larvae induces an increased speed and the maximal distance of macrophage migration in the presence of infection (Fig. 4). These results might indicate that macrophages in the mutant might be less differentiated than those in the wildtype. These factors could contribute to the proliferation of infection.

Since the molecular mechanisms that underlie the role of TLR2 in the control of infection are still unknown we have performed RNAseq of entire larvae with our infection system. We also analyzed the basic expression levels of the mutant versus the control and noted a strong difference of the expression of a large group of genes in the absence of infection. Since little is known about the variations in basal gene expression levels in larvae from different crosses it is hard to speculate whether these differences are related to the Tlr2 mutation. Although we analyzed pools of 10 larvae there are

undoubtedly differences in development of individual larvae that are not filtered away by pooling and that will provide differences in organ development and metabolism that will lead to large variations in gene expression levels. In addition, also differences in the genetic makeup of the parents used for obtaining the batches of larvae are unknown and therefore it will not be possible to obtain solid conclusions. However, the largest category of genes that was significantly affected, namely neurological system process, might still be linked with a function of Tlr2. Many recent studies show that a mutation in Tlr2 in mice resulted in effects of neuronal development and responses to injury (56, 57). Some of these studies show a connection of Tlr2 in neuronal defects to be related to IL10 and possibly autophagy (58, 59). When focusing on the possible signaling pathways that could be involved we observed that there was a significant effects in the GO category of transcriptions factor, namely the c-Maf factors that totals up to 546 representatives that were affected (Supplementary Table 4). As members of Maf family transcription factors, c-Maf and Mafb are specifically expressed in monocyte and macrophage lineages (60, 61), in addition, c-Maf is also expressed in T helper cells (61). c-Maf was also reported to directly regulate IL-10 expression induced by LPS in macrophages (62). Double deficiency of Mafb/c-Maf promotes self-renewal of differentiated macrophages (63), which might indicate a link to the effect of the Tlr2 mutation on the number of macrophages in the absence of infection.

An analysis of the difference of induction and repression of genes during infection showed that that is a very pronounced effect of mutation of the Tlr2 gene. With respect to the number of genes affected, The strongest effect was observed on the genes that are down regulated during infection, since this category was strongly affected in the Tlr2 mutant (Fig. 6A, B). This category of genes includes several genes that are related to innate immune response and also many unknown genes. This indicates that Tlr2 has an important function in anti-inflammatory responses. This is in line with previous reports of studies in mice that showed a strongly decreased anti-inflammatory response in Tlr2 knockouts (64, 65). In a further analysis on the quantitative effects on the differences in expression levels of the genes that are affected in both the up regulated as down regulated groups we selected a group of genes that were most significantly affected for Gene Ontology analysis (Fig. 6D, E). This GO analysis showed many groups to be affected with the immune response as the biggest group. We also performed GSEA and SNEA analyses showing that the *tlr2*-/- mutant has a very different immune response than the heterozygote control line and that many signaling pathways that are linked to responses to human tuberculosis infection are differently responding. Most significantly, activation of the Tlr8 pathway was strongly affected (Fig. S7). This suggests that the Tlr2 signaling is strongly connected with Tlr8 function. TLR8 mutations (polymorphisms) increase susceptibility to mycobacteria (66, 67). These predictions from integrated transcriptome analysis are very valuable, and we would like to study them in our future work. In addition to

known immune genes we want to discuss three other very interesting categories of genes.

The vitamin D receptor pathway genes that are normally up-regulated during infection in zebrafish larvae were down regulated in the Tlr2 mutant. Furthermore, pathway analysis (Fig. S5 and S7) also implicated the expression of the Tlr8 pathway connected to vitamin D signaling as being strongly affected in the Tlr2 mutant. Vitamin D has been shown to be an important regulatory factor during tuberculosis (68) and has been linked previously to TLR2 function in studies in cell cultures (69).

Tlr2 showed to be essential for the up-regulation of a group of genes that encode the Diverse Immunoglobulin Domain-Containing Proteins (DICPS). This group is as novel multigene family encoding diversified immune receptors. Haire et al (70) reported that recombinant DICP Ig domains bind lipids and lipid extracts of different bacteria, including Mtb and Mm, a property shared by mammalian CD300 and TREM family members. In the down-regulated set also several DICP proteins appear to be dependent on Tlr2, such as *dicp1.17*, *dicp3.3*, that are linked to the GO term insulin-like growth factor binding. These correlations might relate to functions of TLR2 in other processes such as the control of diabetes type II by gut microbiota. However, the DICP gene family lacks easily recognizable genetic orthologues in mammals, making a translation to a function in mammalian tuberculosis and other diseases currently not yet possible (71).

Another highly relevant large category of genes of which the induction or repression during infection is dependent on Tlr2 includes the chemokines. In a previous study of our laboratory, Torraca et al. (40) demonstrated the function of the CXCR3-CXCL11 axis in macrophage recruitment and showed that disruption of this axis by *cxcr3.2*-mutation increases the resistance to mycobacterial infection. They also showed that Cxcr3.2 deficiency limited the macrophage-mediated dissemination of mycobacteria and attenuated the formation of granulomatous lesions and led to a reduction in the total bacterial burden (40). In our study, the *tlr2* mutant shows a significantly lower expression of *cxcl11aa* and *cxcl11ac* during Mm infection (Fig. 5). Considering the large number of other chemokines that are controlled by Tlr2 during infection, it is clear that the integrative network of connections cannot yet be understood from these expression studies and need more detailed functional analyses, e.g. by combinations of different mutations or directed studies on responses to chemokines as shown by Torraca et al. However, we can state that the phenotypes of the *tlr2* mutant, at the microscopic level, and the level of transcriptional control such as the mentioned effects on regulation of MafB/c-Maf and chemokines shows a clear connection with macrophage migration. This does not exclude that Tlr2 has many other functions in macrophage behavior during infection such as phagocytosis. For instance, Blander et al. (72) and Rahman et al. (73) showed that phagocytosis of bacteria and phagosome

maturation are impaired in the absence of TLR signaling. Therefore, the large number of unannotated genes of which the expression during infection is dependent on Tlr2 is also worth studying in more detail in future studies.

In conclusion, our study shows that TLR2, as a part of innate immunity, plays an important role in controlling mycobacterial infection as observed on the transcriptome and infection level. This may be mediated by several strategies, including macrophage migration and clustering, and other anti-mycobacterial effect like vitamin D signaling. The anti-inflammatory function of TLR2 as indicated by our study could be mediated by IL10. The gene *il10* is also controlled by other bacteria, yeasts or viruses to mediate immune evasion through TLR2 and therefore seems to have an opposing function as to what we report for mycobacterial infection (25, 26, 74). The TLR2 mutant is therefore highly suitable for further studies using the published infection models for other microbes and viruses in zebrafish larvae. This will make it possible to compare the possibly different roles of TLR2 in interactions with various microbes in one infection model.

Materials and methods

Zebrafish husbandry

The *tlr2*^{sa19423} mutant line (ENU-mutagenized) was obtained from the Sanger Institute Zebrafish Mutation Resource (Hinxton, Cambridge, UK) and shipped by the zebrafish resource Center of the Karlsruhe Institute of Technology. The mutant allele was identified by sequencing. Heterozygous carriers of the mutation were outcrossed twice against wildtype (*AB* strain), and were subsequently incrossed twice. Heterozygous fish of the resulting family were used to produce embryos. Homozygous mutants were outcrossed to the *Tg*(*mpeg1:EGFP*)^{gl22} transgenic line, and the offspring with GFP florescence were subsequently incrossed to produce *tlr2*$^{-/-}$ / *Tg*(*mpeg1:EGFP*) line.

All zebrafish were handled in compliance with the local animal welfare regulations and maintained according to standard protocols (zfin.org). Larvae were raised in egg water (60 g/ml Instant Ocean sea salts) at 28.5 °C. For the duration of bacterial injections, larvae were kept under anesthesia in egg water containing 0.02% buffered 3-aminobenzoic acid ethyl ester (Tricaine, Sigma-Aldrich, the Netherlands). The culture of zebrafish with mutations in immune genes was approved by the local animal welfare committee (DEC) of the University of Leiden (protocol 14198). All protocols adhered to the international guidelines specified by the EU Animal Protection Directive 2010/63/EU.

Bacterial strain preparation

The bacterial strain, *Mycobacterium marinum* m20 (Mma20) expressing mCherry fluorescent protein (75), was used in this study. For the infection to zebrafish larvae, the bacteria were prepared as previously described (76). The infection inoculum was prepared in 2% polyvinylpyrrolidone40 solution (CalBiochem, the Netherlands), and 150 colony-forming units (CFU) of bacteria were injected into the blood stream at 28 hours post fertilization (hpf) as previously described (77).

Ligands injection

Purified Pam3CSK4 (InvivoGen, France) and flagellin from *S. typhimurium* (Flagellin FliC VacciGrade™, Invitrogen, France) were diluted in 1 mg/ml and 100 µg/ml in sterile water, respectively. For injection, 1 nl of the ligand solutions were injected into the blood stream at 28hpf. Sterile water was injected as a control experiment. Injections were performed using a FemtoJet microinjector (Eppendorf, the Netherlands) equipped with a capillary glass needle.

Morpholino injection

Morpholino oligonucleotides (Gene Tools, Philomath, US) were diluted to desired concentrations in 1× Danieau's buffer (58 mM NaCl, 0.7 mM KCl, 0.4 mM $MgSO_4$, 0.6 mM $Ca(NO_3)_2$, 5.0 mM HEPES[pH 7.6]) containing 1× phenol red (Sigma-Aldrich, the Netherlands). For knockdown experiments, *tlr2* ATG-morpholino (*tlr2* mo, 5'-AGTCATTG TTCCTACGAGTCTCATC-3') was injected with the optimal concentration at 0.5mM and 1nl volume per embryo at 1-2 cell stages. Control larvae were injected with the standard control morpholino (Ctrl mo, 5'-CCTCTTACCTCAGTTACAATTTA TA-3').

Immunohistochemistry

Larvae were fixed in 4% paraformaldehyde in PBS overnight at 4°C. Myeloperoxidase (Mpx) activity was labeled using TSA-Plus Systems (Perkin Elmer, Waltham, MA, US) as previously described (78).

Imaging and quantification of bacterial loads

Pools of 20 larvae were collected at 3- and 4-day post infection (dpi) and imaged by using the Leica MZ16FA Fluorescence Stereo Microscope (Leica Microsystems, info) equipped with the Leica DC500 camera (Leica Microsystems). Bacterial loads were analyzed using dedicated pixel counting software as previously described (79). Experiments were performed in triplicate.

Confocal microscopy imaging

Larvae (4 or 5 dpf) were embedded in 1% low melting point agarose (Sigma Aldrich), and image acquisition was performed by using a Leica TCS SPE confocal microscope

(Leica Microsystems) or a Zeiss LSM exciter on an Axio Observer confocal microscope (info) with 10 or 63 times objectives. Acquisition settings and area of imaging (in the caudal vein region) were kept the same across the groups for quantification of the bacterial burden.

Macrophage tracking

To visualize the granuloma formation and the leukocyte phenotype, *tlr2*$^{-/-}$ zebrafish were crossed with macrophage-specific reporter line *Tg*(*mpeg1:EGFP*), leading to *tlr2*$^{+/+}$/*Tg*(*mpeg1:EGFP*) and *tlr2*$^{-/-}$*Tg*(*mpeg1:EGFP*) fish lines. *tlr2*$^{+/+}$ and *tlr2*$^{-/-}$ - *Tg(mpeg1:EGFP)* embryos were injected with 150 CFU Mma20 at 1dpf. They were anesthetized and mounted in 1% low-melting agarose and subsequently imaged using a Nikon Eclipse Ti-E inverted microscope (40×) as described previously (80) from 84 hpi to 96 hpi. Images were taken every 6.5 min, extracted, and converted to movies using NIS-Elements AR software. ImageJ (NIH, Bethesda, ML, USA) was used to align all the frames. CellTracker (ver. 1.1, Copyright (©) 2015 Peter Horvath and Filippo Piccinini) was employed to analyze the moving tracks of infected macrophages.

RNA isolation, cDNA synthesis and qPCR

Total RNAs were extracted using TRIzol Reagent (Life Technologies) and purified using RNeasy MinElute Cleanup Kit (Qiagen, the Netherlands). The concentration and quality of RNAs were evaluated by NanoDrop 2000 (Thermo Scientific, the Netherlands). cDNAs were synthesized from 1 µg total RNAs and qPCR were performed by using the iScript™ cDNA Synthesis Kit (BioRad, the Netherlands) and iQ™ SYBR Green Supermix (BioRad) and normalized against the expression of *ppial* as a housekeeping gene (81). Results were analyzed using the ΔΔCt method (82). Primer sequences are described in Supplementary Table 1.

Deep sequencing and data analysis

Triplicates of 10 larvae of *tlr2*$^{+/-}$ and *tlr2*$^{-/-}$ with PBS (as control) or Mma20 injection, were homogenized in 300ul of TRIzol reagent, and total RNAs were purified as described above. RNAseq was performed using Illumina Hi-Seq 2500 as previously described (83). The RNAseq data were mapped on zebrafish genome (GRCz10 version) and tag counts were performed by Bowtie 2 using GeneTiles software (http://www.genetiles. com) (84, 85). Then, we performed normalization and gene expression analysis using the R package and DESeq2 (86). After statistical tests, we performed further bioinformatics analyses Gene-Set Enrichment Analysis (42), Sub-Network Enrichment Analysis (43) and Pathway Enrichment Analysis (87). For creating gene networks based on common regulatory targets, we used Pathway Studio 9.0 (Elsevier, Amsterdam, the Netherlands) as previously described (41).

Acknowledgments

We thank all members of the fish facility team for fish caretaking. We would like to thank Lanpeng Chen and Gerda E.M. Lamers for assistance with confocal imaging. We also thank to Vincenzo Torraca for helpful discussions and the qPCR primers of *cxcl11*-like genes. S. Y. was supported by a grant from the China Scholarship Council (CSC).

The zebrafish Tlr2 mutant was obtained from the Sanger Institute Zebrafish Mutation Resource (ZF-MODELS Integrated Project funded by the European Commission; contract number LSHG-CT-2003-503496), also sponsored by the Welcome Trust [grant number WT 077047/Z/05/Z].

Supplementary data

Supplementary figure 1 Relative pixel count analysis for TSA staining of neutrophils in 2dpf *tlr2*$^{+/-}$ and *tlr2*$^{-/-}$ embryos.

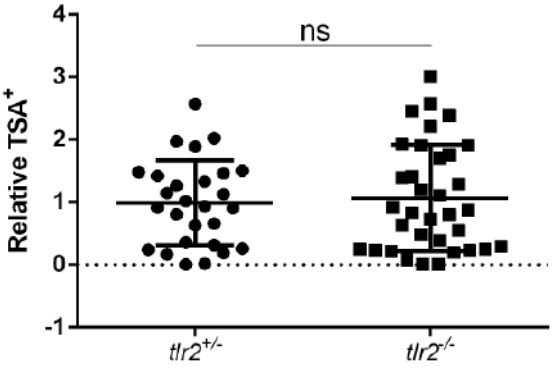

Supplementary figure 2 *tlr2*-dependent up regulation of other process related specific genes.

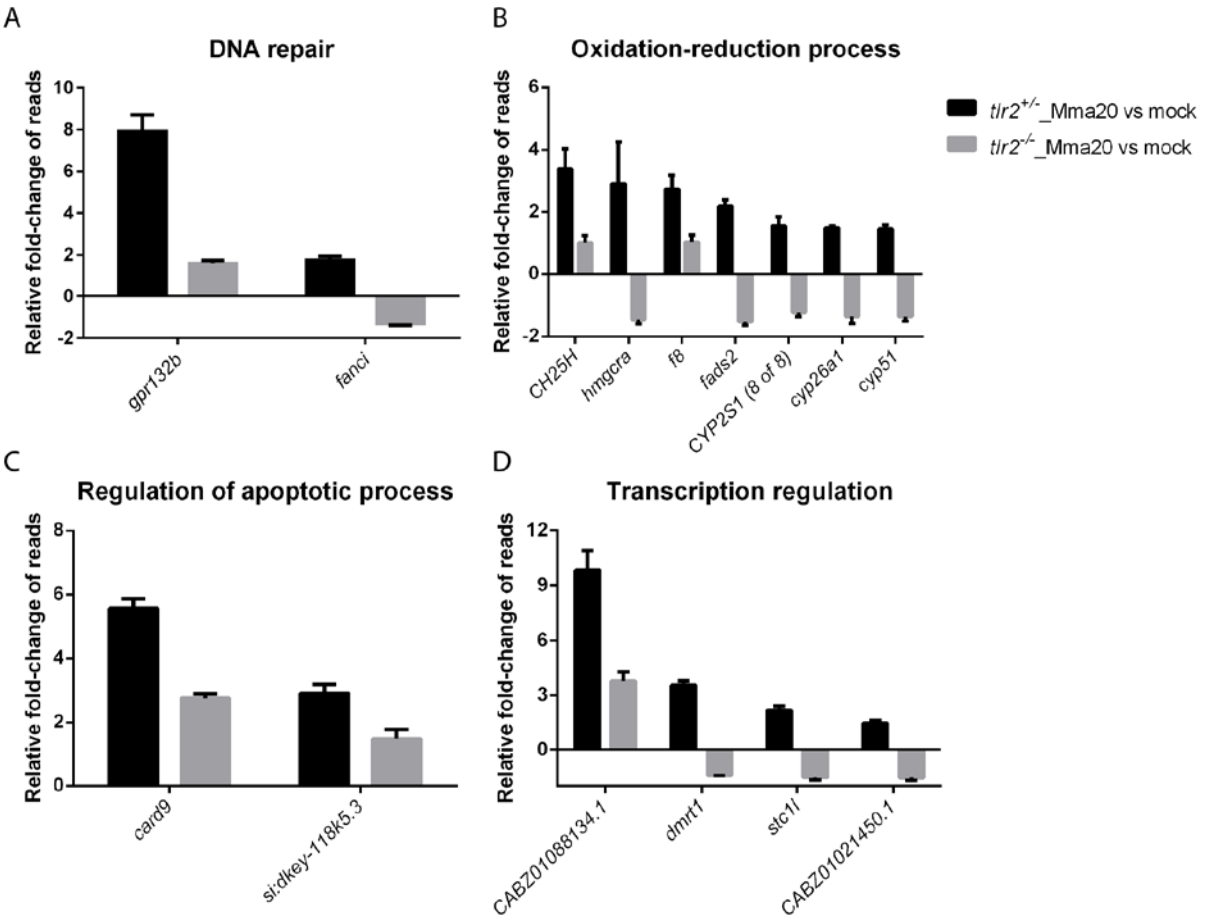

Supplementary figure 3 *tlr2*-dependent down regulation of other process related specific genes.

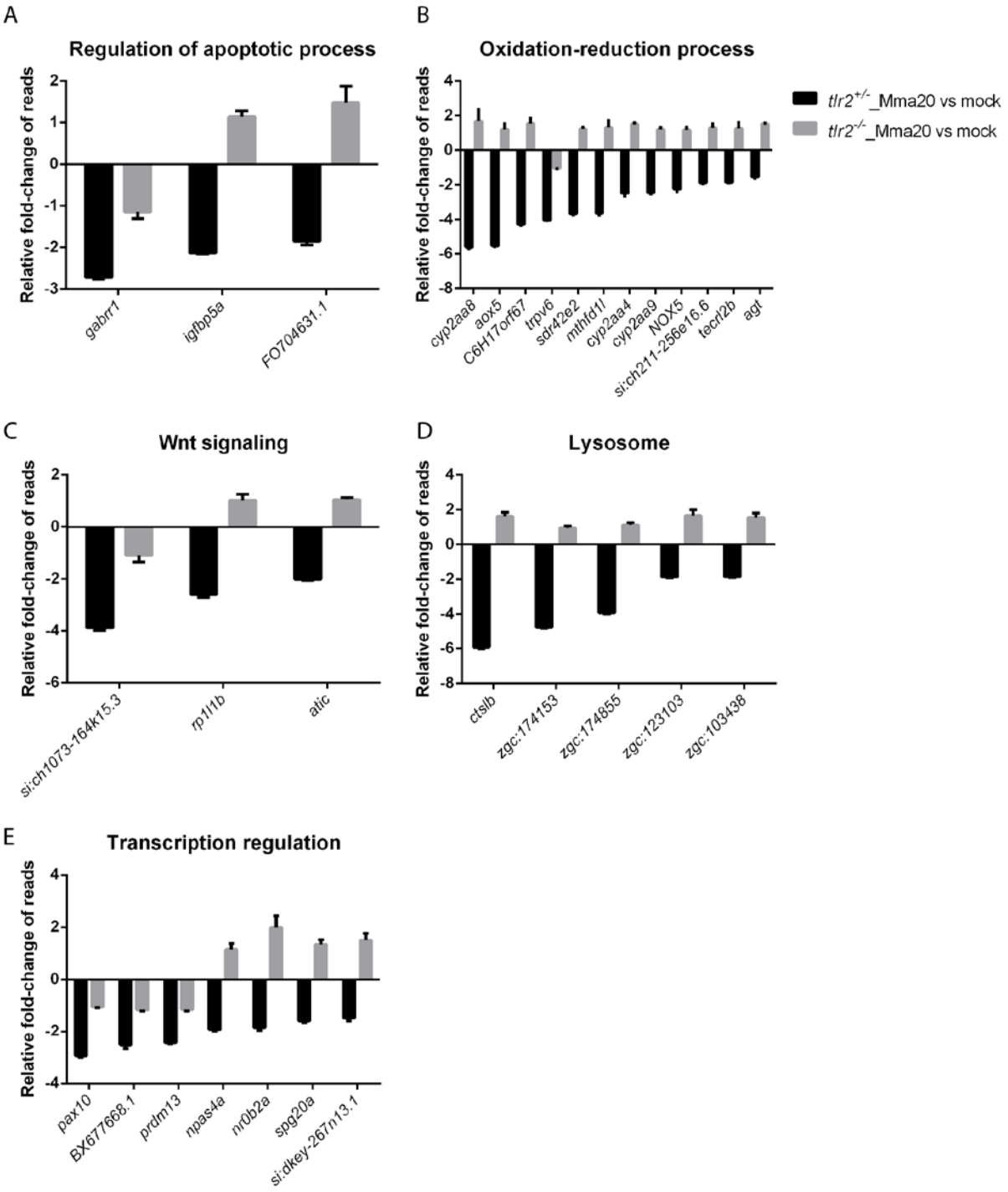

Supplementary figure 4 Representative images of Fig. 1D and 1E. Green signal represents macrophages, red signal represents neutrophils.

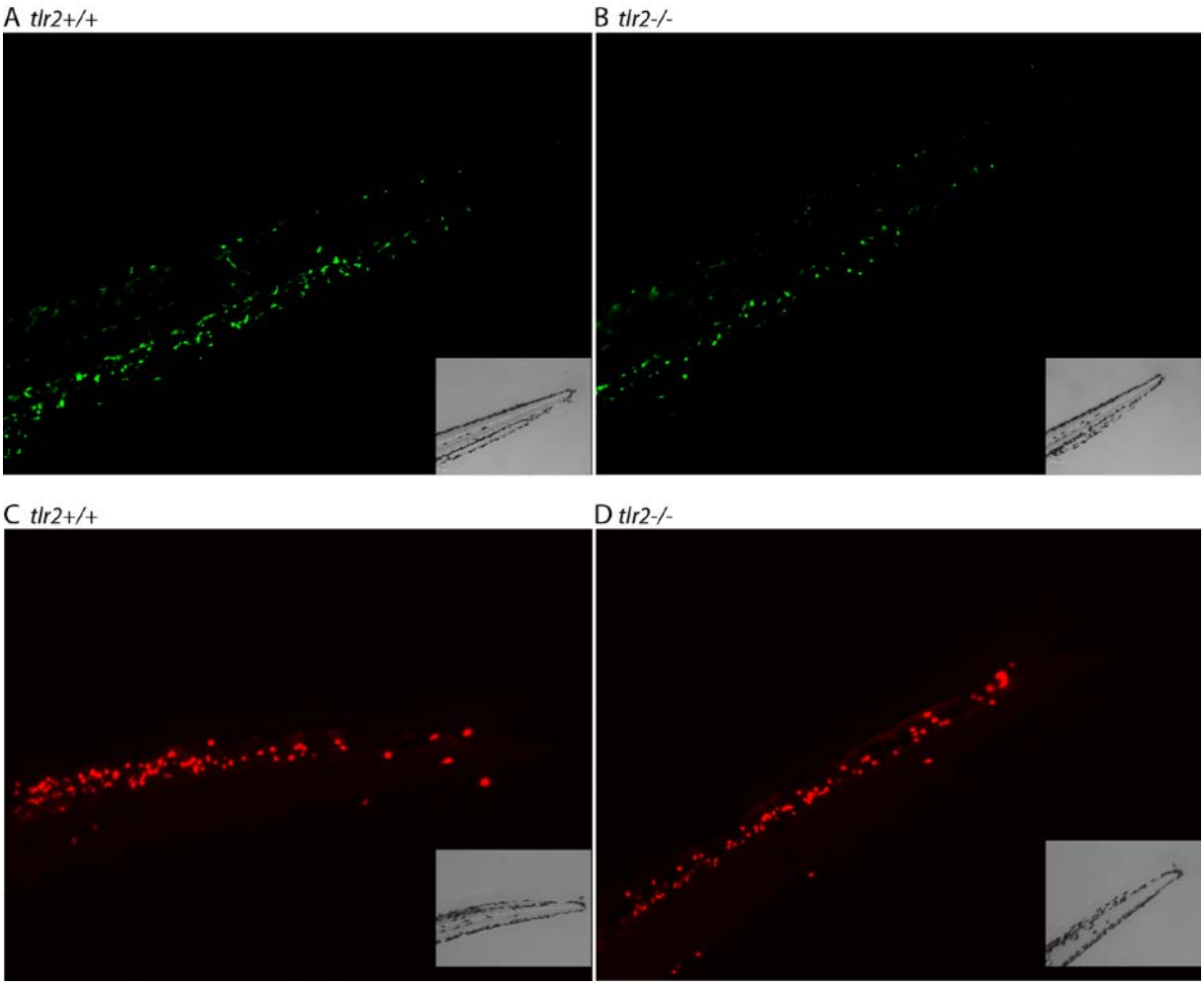

Supplementary figure 5 Sub-network enrichment analysis. The networks of common targets of the 97 up regulated genes (Fig.6D) in *tlr2*$^{+/-}$ (A) and *tlr2*$^{-/-}$ (B) with Mma20 infection. Red represents up regulation, blue represents down regulation and grey represents genes for which no expression was detected.

A

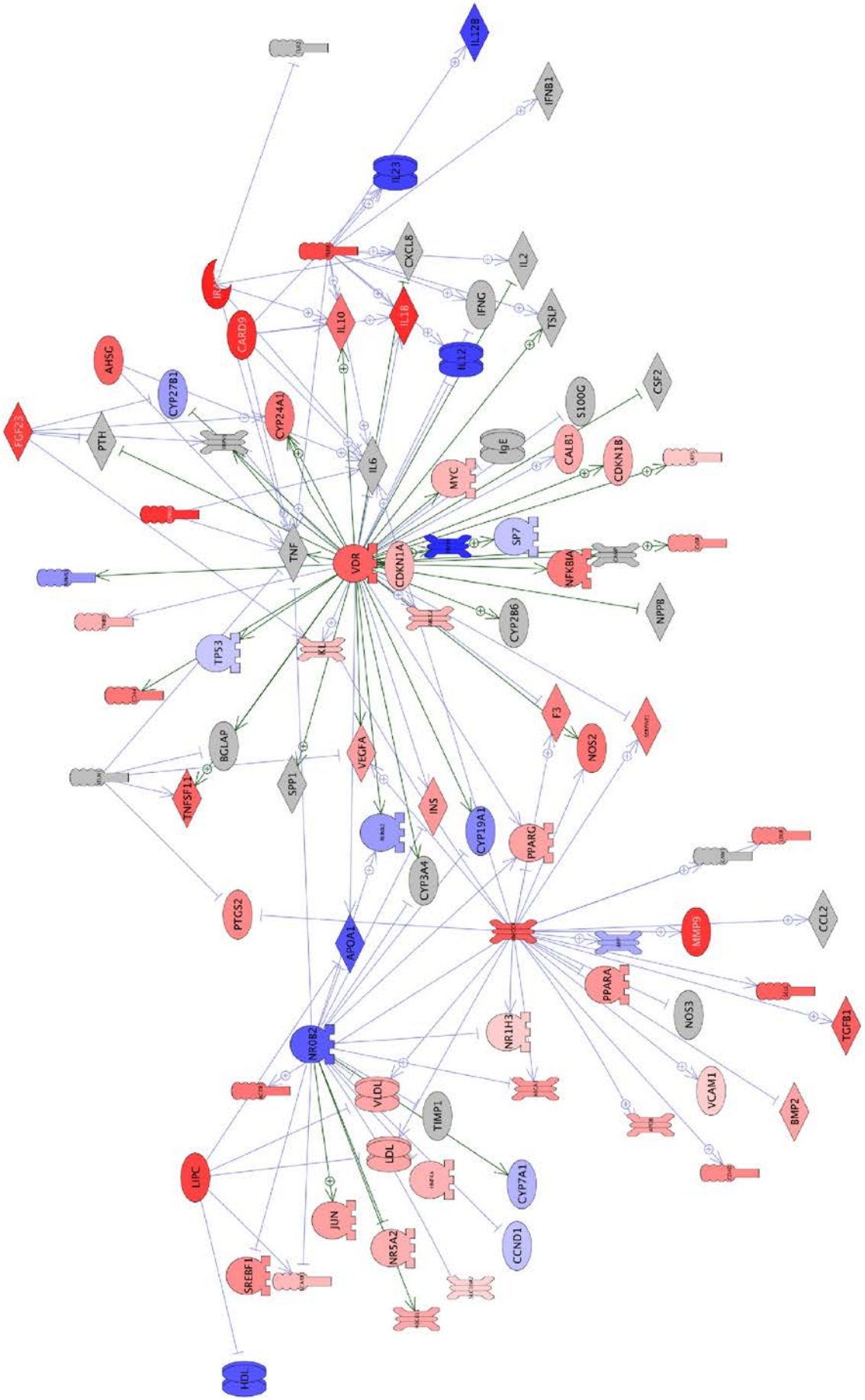
IL12B
IFNB1
IL23
CXCL8
IL2
IRAK
IL10
IL18
IFNG
TSLP
CARD9
IL12
AHSG
CYP27B1
CSF2
S100G
FGF23
PTH
CYP24A1
IgE
CALB1
CDKN1B
IL6
MYC
TNF
VDR
CDKN1A
SP7
NFKBIA
NPPB
CYP2B6
TP53
KL
F3
NOS2
BGLAP
VEGFA
SPP1
TNFSF11
INS
CYP19A1
PPARG
CYP3A4
PTGS2
APOA1
MMP9
CCL2
PPARA
NOS3
TGFB1
NR1H3
NR0B2
VLDL
VCAM1
BMP2
TIMP1
LDL
LIPC
CYP7A1
JUN
CCND1
NR5A2
SREBF1
HDL

B

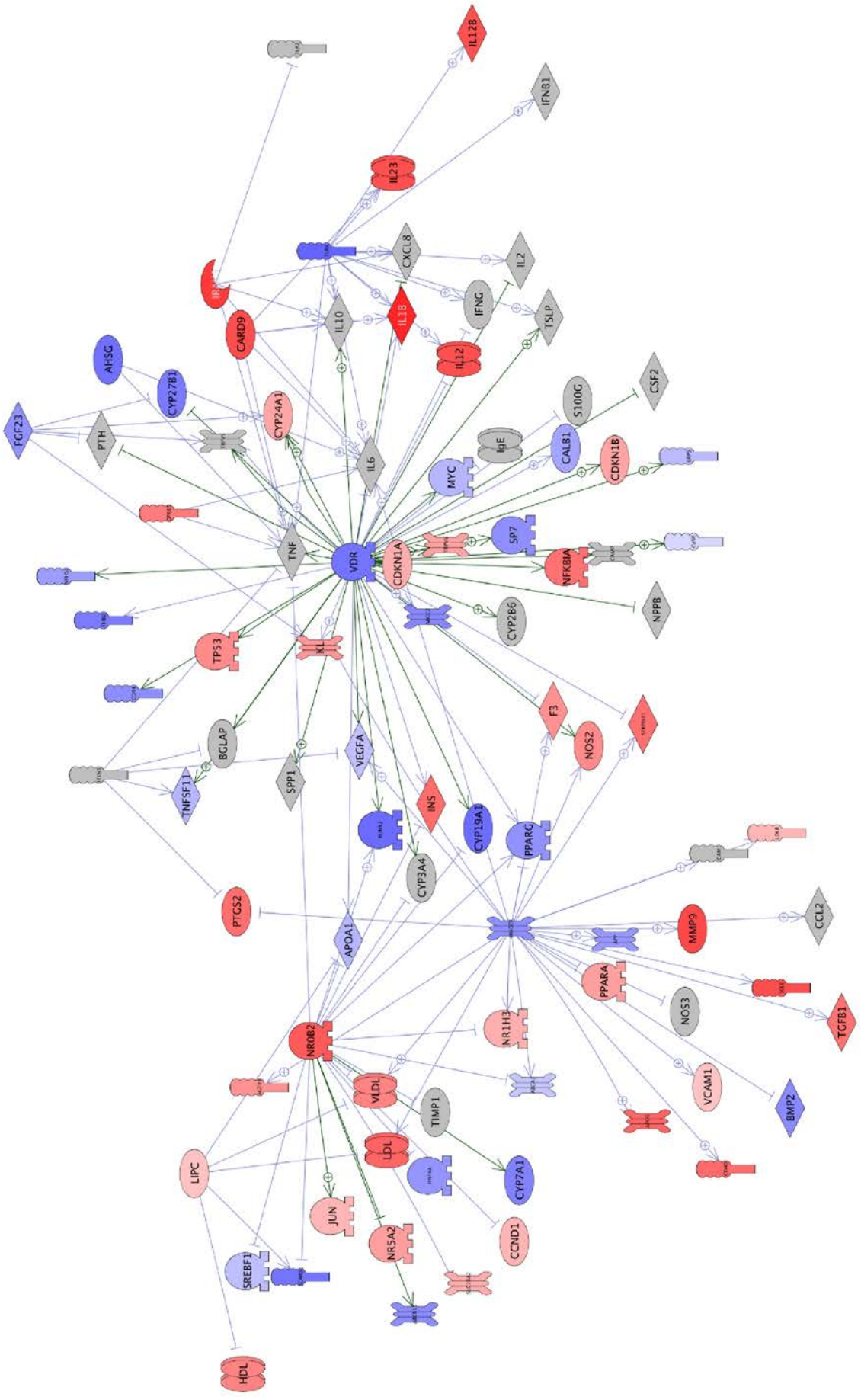
IL12B
IFNB1
IL23
CXCL8
IL2
IFNG
TSLP
IL18
IL12
IL10
CARD9
AHSG
CYP27B1
FGF23
PTH
CYP24A1
IL6
MYC
IgE
CAL81
S100G
CSF2
CDKN1B
TNF
VDR
CDKN1A
SP7
NFKBIA
NPPB
CYP2B6
TP53
KL
BGLAP
TNFSF11
SPP1
VEGFA
INS
CYP19A1
PPARG
F3
NOS2
CYP3A4
PTGS2
APOA1
MMP9
CCL2
PPARA
NOS3
TGFB1
NR1H3
NR0B2
VLDL
TIMP1
VCAM1
BMP2
LDL
LIPC
CYP7A1
JUN
NR5A2
CCND1
SREBF1
HDL

Supplementary figure 6 Sub-network enrichment analysis. The networks of the common targets of the 92 down regulated genes (Fig. 6E) in *tlr2*$^{+/-}$ (A) and *tlr2*$^{-/-}$ (B) with Mma20 infection. Red represents up-regulation, blue represents down-regulation and grey represents genes for which no expression was detected.

A

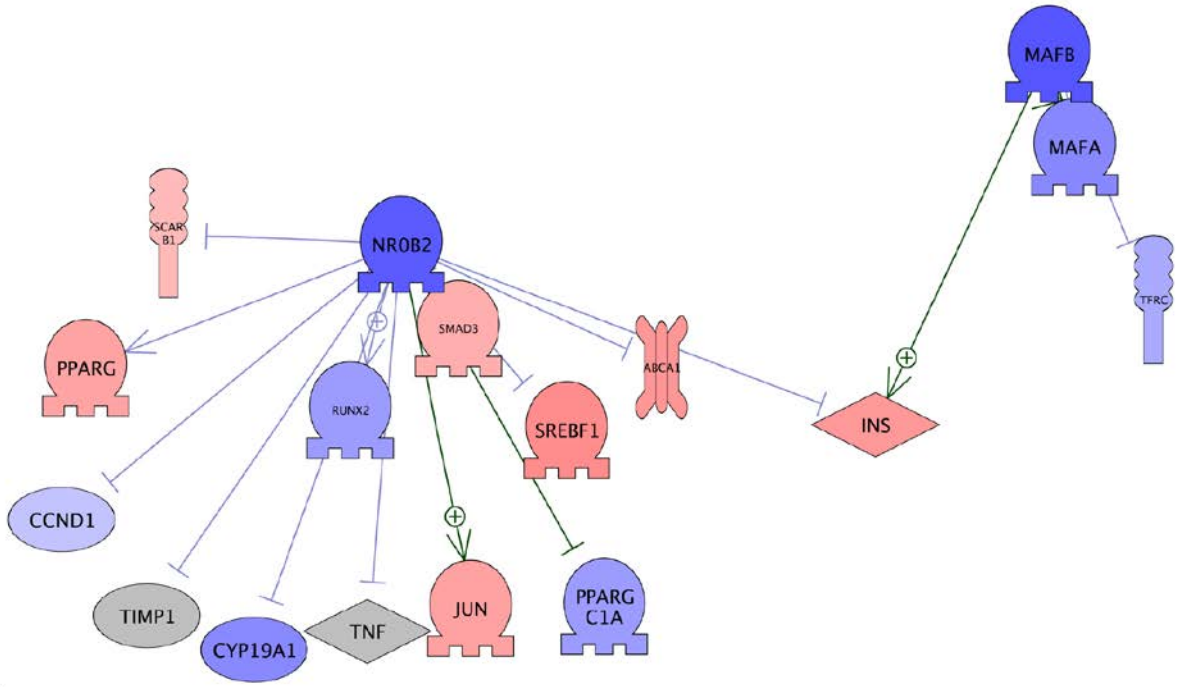

B

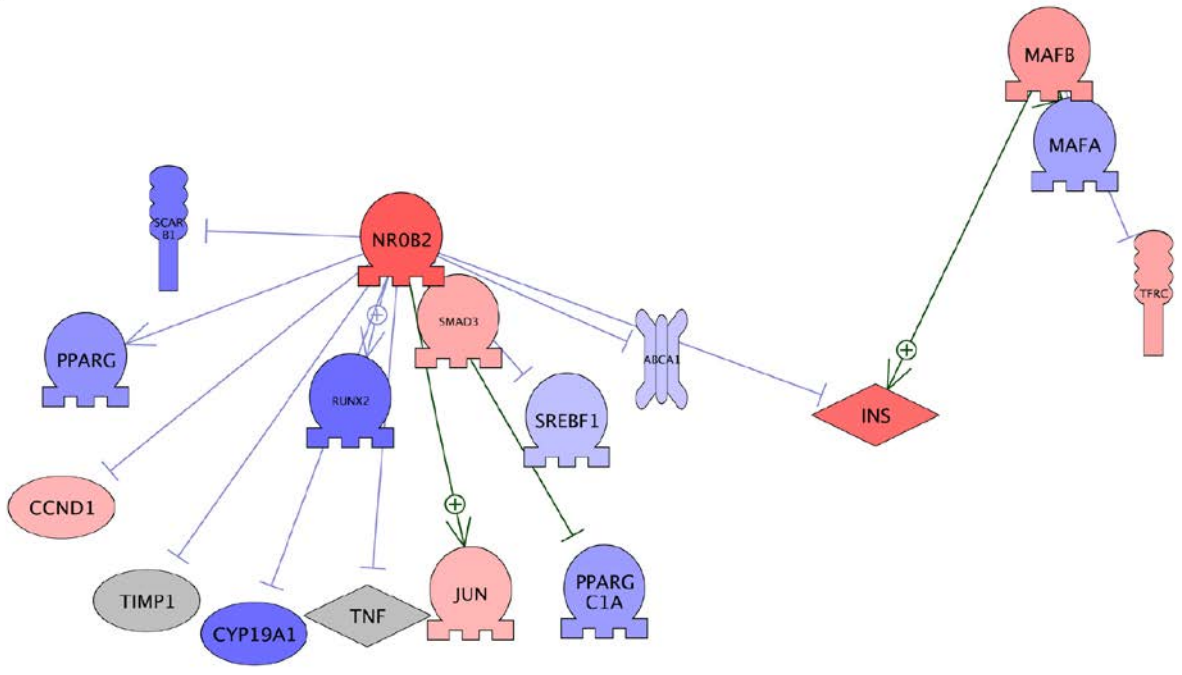

Supplementary figure 7 Sub-network enrichment analysis between zebrafish and human. The Tlr8 pathway in zebrafish (A) with Mm infection and human macrophages (B) with Mtb infection. Red represents up-regulation, blue represents down-regulation

A

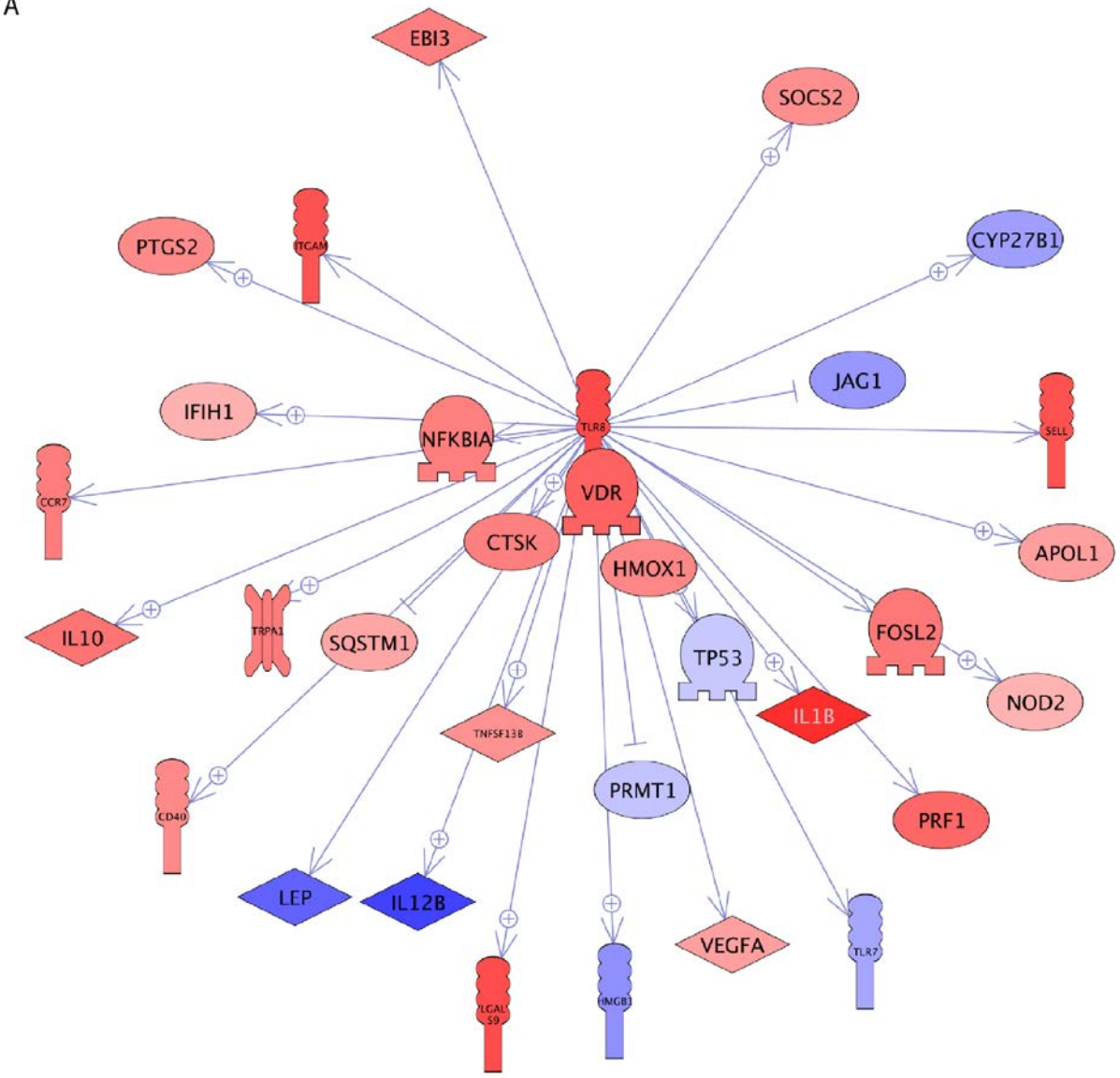

B

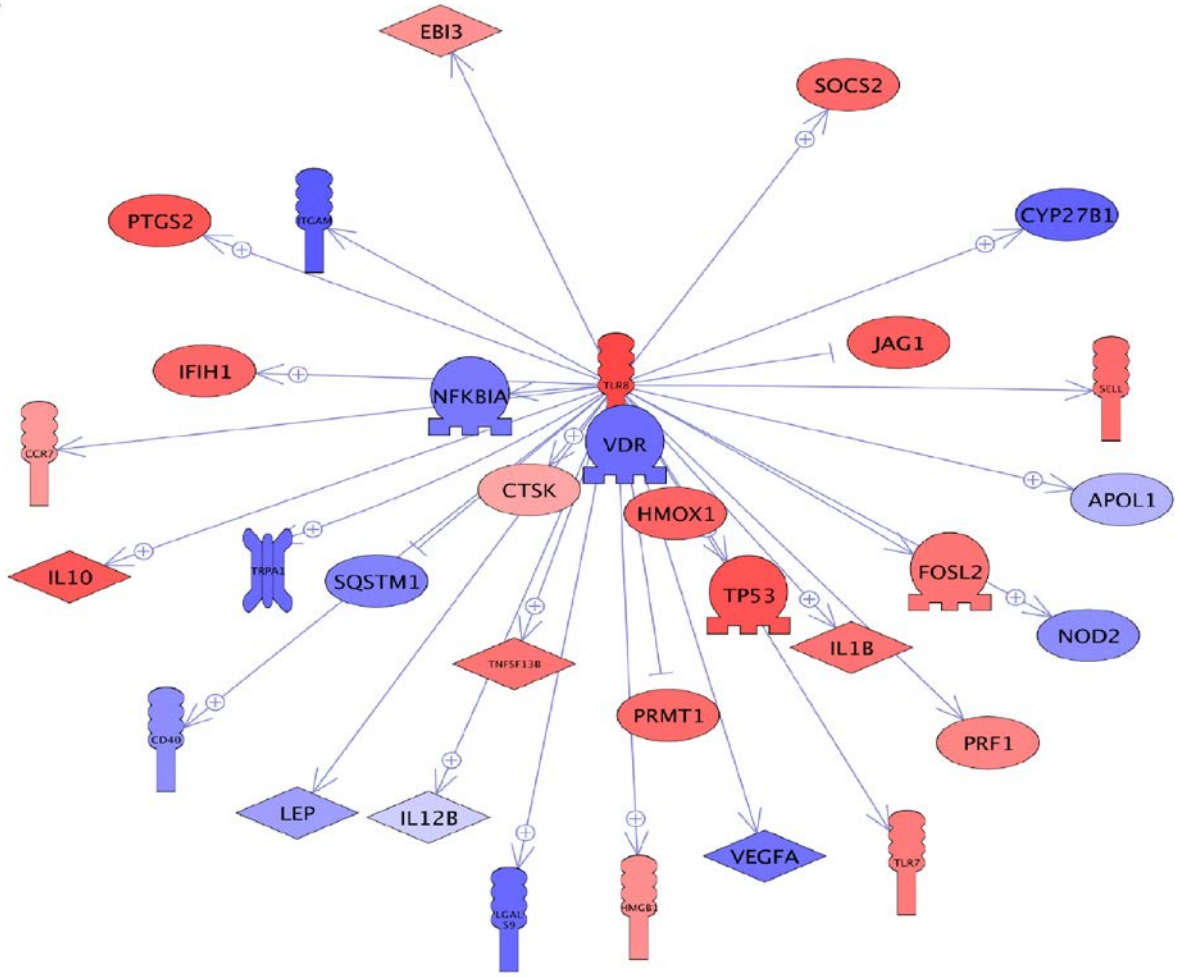

Supplementary Table 1 List of primers

Supplementary Table 2 A-H Gene lists of GSEA and SNEA analysis

Supplementary Table 3 GO analysis of genes that have a different basal expression level in the absence of infection in the Tlr2 mutant versus the heterozygote control. Shown is the GO analysis of the group of 878 genes that were different with a FDR *p* value of 10^{-10} indicated in Fig. 6F.

Supplementary Table 4 List of transcription factors under GO category in absence of infection

Supplementary Table 5 List of basal expression levels of gene *mpx* and *mpeg1*

References

1. Co, D. O., L. H. Hogan, S. I. Kim, and M. Sandor. 2004. Mycobacterial granulomas: keys to a long-lasting host-pathogen relationship. *Clin Immunol* 113: 130-136.
2. Salgame, P. 2005. Host innate and Th1 responses and the bacterial factors that control Mycobacterium tuberculosis infection. *Current opinion in immunology* 17: 374-380.
3. Jo, E. K., C. S. Yang, C. H. Choi, and C. V. Harding. 2007. Intracellular signalling cascades regulating innate immune responses to Mycobacteria: branching out from Toll-like receptors. *Cell Microbiol* 9: 1087-1098.
4. Tapping, R. I., and P. S. Tobias. 2003. Mycobacterial lipoarabinomannan mediates physical interactions between TLR1 and TLR2 to induce signaling. *J Endotoxin Res* 9: 264-268.
5. Means, T. K., S. Wang, E. Lien, A. Yoshimura, D. T. Golenbock, and M. J. Fenton. 1999. Human toll-like receptors mediate cellular activation by Mycobacterium tuberculosis. *J Immunol* 163: 3920-3927.
6. Means, T. K., B. W. Jones, A. B. Schromm, B. A. Shurtleff, J. A. Smith, J. Keane, D. T. Golenbock, S. N. Vogel, and M. J. Fenton. 2001. Differential effects of a Toll-like receptor antagonist on Mycobacterium tuberculosis-induced macrophage responses. *J Immunol* 166: 4074-4082.
7. Quesniaux, V. J., D. M. Nicolle, D. Torres, L. Kremer, Y. Guerardel, J. Nigou, G. Puzo, F. Erard, and B. Ryffel. 2004. Toll-like receptor 2 (TLR2)-dependent-positive and TLR2-independent-negative regulation of proinflammatory cytokines by mycobacterial lipomannans. *J Immunol* 172: 4425-4434.
8. Jung, S. B., C. S. Yang, J. S. Lee, A. R. Shin, S. S. Jung, J. W. Son, C. V. Harding, H. J. Kim, J. K. Park, T. H. Paik, C. H. Song, and E. K. Jo. 2006. The mycobacterial 38-kilodalton glycolipoprotein antigen activates the mitogen-activated protein kinase pathway and release of proinflammatory cytokines through Toll-like receptors 2 and 4 in human monocytes. *Infect Immun* 74: 2686-2696.
9. Brightbill, H. D., D. H. Libraty, S. R. Krutzik, R. B. Yang, J. T. Belisle, J. R. Bleharski, M. Maitland, M. V. Norgard, S. E. Plevy, S. T. Smale, P. J. Brennan, B. R. Bloom, P. J. Godowski, and R. L. Modlin. 1999. Host defense mechanisms triggered by microbial lipoproteins through toll-like receptors. *Science* 285: 732-736.
10. Noss, E. H., R. K. Pai, T. J. Sellati, J. D. Radolf, J. Belisle, D. T. Golenbock, W. H. Boom, and C. V. Harding. 2001. Toll-like receptor 2-dependent inhibition of macrophage class II MHC expression and antigen processing by 19-kDa lipoprotein of Mycobacterium tuberculosis. *J Immunol* 167: 910-918.
11. Gilleron, M., V. F. Quesniaux, and G. Puzo. 2003. Acylation state of the phosphatidylinositol hexamannosides from Mycobacterium bovis bacillus Calmette Guerin and mycobacterium tuberculosis H37Rv and its implication in Toll-like receptor response. *J Biol Chem* 278: 29880-29889.
12. Gilleron, M., J. Nigou, D. Nicolle, V. Quesniaux, and G. Puzo. 2006. The acylation state of mycobacterial lipomannans modulates innate immunity response through toll-like receptor 2. *Chem Biol* 13: 39-47.
13. Takeuchi, O., S. Sato, T. Horiuchi, K. Hoshino, K. Takeda, Z. Dong, R. L. Modlin, and S. Akira. 2002. Cutting edge: role of Toll-like receptor 1 in mediating immune response to microbial lipoproteins. *J Immunol* 169: 10-14.
14. Takeuchi, O., T. Kawai, P. F. Mühlradt, M. Morr, J. D. Radolf, A. Zychlinsky, K. Takeda, and S. Akira. 2001. Discrimination of bacterial lipoproteins by Toll-like receptor 6. *Int Immunol* 13: 933-940.
15. Marinho, F. A. V., R. R. de Paula, A. C. Mendes, L. A. de Almeida, M. T. R. Gomes, N. B. Carvalho, F. S. Oliveira, M. V. Caliari, and S. C. Oliveira. 2013. Toll-like receptor 6 senses Mycobacterium avium and is required for efficient control of mycobacterial infection. *Eur J Immunol* 43: 2373-2385.
16. Basu, J., D. M. Shin, and E. K. Jo. 2012. Mycobacterial signaling through toll-like receptors. *Front Cell Infect Microbiol* 2: 145.
17. Underhill, D. M., A. Ozinsky, K. D. Smith, and A. Aderem. 1999. Toll-like receptor-2 mediates mycobacteria-induced proinflammatory signaling in macrophages. *Proc Natl Acad Sci U S A* 96: 14459-14463.
18. Carlos, D., F. G. Frantz, D. A. Souza-Junior, M. C. Jamur, C. Oliver, S. G. Ramos, V. F. Quesniaux, B. Ryffel, C. L. Silva, M. T. Bozza, and L. H. Faccioli. 2009. TLR2-dependent mast cell activation contributes to the control of Mycobacterium tuberculosis infection. *Microbes Infect* 11: 770-778.
19. Reiling, N., C. Holscher, A. Fehrenbach, S. Kroger, C. J. Kirschning, S. Goyert, and S. Ehlers. 2002. Cutting edge: Toll-like receptor (TLR)2- and TLR4-mediated pathogen recognition in resistance to airborne infection with Mycobacterium tuberculosis. *J Immunol* 169: 3480-3484.
20. Drennan, M. B., D. Nicolle, V. J. Quesniaux, M. Jacobs, N. Allie, J. Mpagi, C. Fremond, H. Wagner, C. Kirschning, and B. Ryffel. 2004. Toll-like receptor 2-deficient mice succumb to Mycobacterium tuberculosis infection. *Am J Pathol* 164: 49-57.
21. Noss, E. H., C. V. Harding, and W. H. Boom. 2000. Mycobacterium tuberculosis inhibits MHC class II antigen processing in murine bone marrow macrophages. *Cell Immunol* 201: 63-74.
22. Gehring, A. J., K. M. Dobos, J. T. Belisle, C. V. Harding, and W. H. Boom. 2004. Mycobacterium tuberculosis LprG (Rv1411c): a novel TLR-2 ligand that inhibits human macrophage class II MHC antigen processing. *J Immunol* 173: 2660-2668.
23. Saraav, I., S. Singh, and S. Sharma. 2014. Outcome of Mycobacterium tuberculosis and Toll-like receptor interaction: immune response or immune evasion? *Immunol Cell Biol* 92: 741-746.
24. Netea, M. G., J. W. Van der Meer, and B. J. Kullberg. 2004. Toll-like receptors as an escape mechanism from the host defense. *Trends Microbiol* 12: 484-488.

25. Netea, M. G., R. Sutmuller, C. Hermann, C. A. Van der Graaf, J. W. Van der Meer, J. H. van Krieken, T. Hartung, G. Adema, and B. J. Kullberg. 2004. Toll-like receptor 2 suppresses immunity against Candida albicans through induction of IL-10 and regulatory T cells. *J Immunol* 172: 3712-3718.
26. Sing, A., D. Rost, N. Tvardovskaia, A. Roggenkamp, A. Wiedemann, C. J. Kirschning, M. Aepfelbacher, and J. Heesemann. 2002. Yersinia V-antigen exploits toll-like receptor 2 and CD14 for interleukin 10-mediated immunosuppression. *J Exp Med* 196: 1017-1024.
27. Gehring, A. J., R. E. Rojas, D. H. Canaday, D. L. Lakey, C. V. Harding, and W. H. Boom. 2003. The Mycobacterium tuberculosis 19-kilodalton lipoprotein inhibits gamma interferon-regulated HLA-DR and Fc gamma R1 on human macrophages through Toll-like receptor 2. *Infect Immun* 71: 4487-4497.
28. Alvarez, G. R., B. S. Zwilling, and W. P. Lafuse. 2003. Mycobacterium avium inhibition of IFN-gamma signaling in mouse macrophages: Toll-like receptor 2 stimulation increases expression of dominant-negative STAT1 beta by mRNA stabilization. *J Immunol* 171: 6766-6773.
29. Agrawal, S., A. Agrawal, B. Doughty, A. Gerwitz, J. Blenis, T. Van Dyke, and B. Pulendran. 2003. Cutting edge: different Toll-like receptor agonists instruct dendritic cells to induce distinct Th responses via differential modulation of extracellular signal-regulated kinase-mitogen-activated protein kinase and c-Fos. *J Immunol* 171: 4984-4989.
30. Lam, S. H., H. L. Chua, Z. Gong, T. J. Lam, and Y. M. Sin. 2004. Development and maturation of the immune system in zebrafish, Danio rerio: a gene expression profiling, in situ hybridization and immunological study. *Dev Comp Immunol* 28: 9-28.
31. Willett, C. E., A. Cortes, A. Zuasti, and A. G. Zapata. 1999. Early hematopoiesis and developing lymphoid organs in the zebrafish. *Dev Dyn* 214: 323-336.
32. Swaim, L. E., L. E. Connolly, H. E. Volkman, O. Humbert, D. E. Born, and L. Ramakrishnan. 2006. Mycobacterium marinum Infection of Adult Zebrafish Causes Caseating Granulomatous Tuberculosis and Is Moderated by Adaptive Immunity. *Infect Immun* 74: 6108-6117.
33. Davis, J. M., H. Clay, J. L. Lewis, N. Ghori, P. Herbomel, and L. Ramakrishnan. 2002. Real-time visualization of mycobacterium-macrophage interactions leading to initiation of granuloma formation in zebrafish embryos. *Immunity* 17: 693-702.
34. Meijer, A. H. 2015. Protection and pathology in TB: learning from the zebrafish model. *Semin Immunopathol*.
35. Yang, S., R. Marin-Juez, A. H. Meijer, and H. P. Spaink. 2015. Common and specific downstream signaling targets controlled by Tlr2 and Tlr5 innate immune signaling in zebrafish. *BMC Genomics* 16: 547.
36. Medzhitov, R., P. Preston-Hurlburt, E. Kopp, A. Stadlen, C. Chen, S. Ghosh, and C. A. Janeway, Jr. 1998. MyD88 is an adaptor protein in the hToll/IL-1 receptor family signaling pathways. *Mol Cell* 2: 253-258.
37. Fitzgerald, K. A., E. M. Palsson-McDermott, A. G. Bowie, C. A. Jefferies, A. S. Mansell, G. Brady, E. Brint, A. Dunne, P. Gray, M. T. Harte, D. McMurray, D. E. Smith, J. E. Sims, T. A. Bird, and L. A. O'Neill. 2001. Mal (MyD88-adapter-like) is required for Toll-like receptor-4 signal transduction. *Nature* 413: 78-83.
38. Cui, C., E. L. Benard, Z. Kanwal, O. W. Stockhammer, M. van der Vaart, A. Zakrzewska, H. P. Spaink, and A. H. Meijer. 2011. Infectious disease modeling and innate immune function in zebrafish embryos. *Methods Cell Biol* 105: 273-308.
39. Martin, C. J., A. F. Carey, and S. M. Fortune. 2016. A bug's life in the granuloma. *Semin Immunopathol* 38: 213-220.
40. Torraca, V., C. Cui, R. Boland, J.-P. Bebelman, A. M. van der Sar, M. J. Smit, M. Siderius, H. P. Spaink, and A. H. Meijer. 2015. The CXCR3-CXCL11 signaling axis mediates macrophage recruitment and dissemination of mycobacterial infection. *Dis Model Mech* 8: 253-269.
41. Nikitin, A., S. Egorov, N. Daraselia, and I. Mazo. 2003. Pathway studio--the analysis and navigation of molecular networks. *Bioinformatics* 19: 2155-2157.
42. Subramanian, A., P. Tamayo, V. K. Mootha, S. Mukherjee, B. L. Ebert, M. A. Gillette, A. Paulovich, S. L. Pomeroy, T. R. Golub, E. S. Lander, and J. P. Mesirov. 2005. Gene set enrichment analysis: a knowledge-based approach for interpreting genome-wide expression profiles. *Proc Natl Acad Sci U S A* 102: 15545-15550.
43. Kotelnikova, E., A. Yuryev, I. Mazo, and N. Daraselia. 2010. Computational approaches for drug repositioning and combination therapy design. *J Bioinform Comput Biol* 8: 593-606.
44. Verway, M., M. Bouttier, T. T. Wang, M. Carrier, M. Calderon, B. S. An, E. Devemy, F. McIntosh, M. Divangahi, M. A. Behr, and J. H. White. 2013. Vitamin D induces interleukin-1beta expression: paracrine macrophage epithelial signaling controls M. tuberculosis infection. *PLoS Pathog* 9: e1003407.
45. Leisching, G., R. D. Pietersen, V. Mpongoshe, C. van Heerden, P. van Helden, I. Wiid, and B. Baker. 2016. The Host Response to a Clinical MDR Mycobacterial Strain Cultured in a Detergent-Free Environment: A Global Transcriptomics Approach. *PLoS One* 11: e0153079.
46. Kubler, A., C. Larsson, B. Luna, B. B. Andrade, E. P. Amaral, M. Urbanowski, M. Orandle, K. Bock, N. C. Ammerman, L. S. Cheung, K. Winglee, M. Halushka, J. K. Park, A. Sher, J. S. Friedland, P. T. Elkington, and W. R. Bishai. 2016. Cathepsin K Contributes to Cavitation and Collagen Turnover in Pulmonary Tuberculosis. *J Infect Dis* 213: 618-627.
47. Zhang, H., Z. Sun, W. Wei, Z. Liu, J. Fleming, S. Zhang, N. Lin, M. Wang, M. Chen, Y. Xu, J. Zhou, C. Li, L. Bi, and G. Zhou. 2014. Identification of serum microRNA biomarkers for tuberculosis using RNA-seq. *PLoS One* 9: e88909.
48. Mvubu, N. E., B. Pillay, J. Gamieldien, W. Bishai, and M. Pillay. 2016. Canonical pathways, networks and transcriptional factor regulation by clinical strains of Mycobacterium tuberculosis in pulmonary alveolar epithelial cells. *Tuberculosis (Edinb)* 97: 73-85.

49. Vegh, P., D. A. Magee, N. C. Nalpas, K. Bryan, M. S. McCabe, J. A. Browne, K. M. Conlon, S. V. Gordon, D. G. Bradley, D. E. MacHugh, and D. J. Lynn. 2015. MicroRNA profiling of the bovine alveolar macrophage response to Mycobacterium bovis infection suggests pathogen survival is enhanced by microRNA regulation of endocytosis and lysosome trafficking. *Tuberculosis (Edinb)* 95: 60-67.
50. Nalpas, N. C., S. D. Park, D. A. Magee, M. Taraktsoglou, J. A. Browne, K. M. Conlon, K. Rue-Albrecht, K. E. Killick, K. Hokamp, A. J. Lohan, B. J. Loftus, E. Gormley, S. V. Gordon, and D. E. MacHugh. 2013. Whole-transcriptome, high-throughput RNA sequence analysis of the bovine macrophage response to Mycobacterium bovis infection in vitro. *BMC Genomics* 14: 230.
51. Casey, M. E., K. G. Meade, N. C. Nalpas, M. Taraktsoglou, J. A. Browne, K. E. Killick, S. D. Park, E. Gormley, K. Hokamp, D. A. Magee, and D. E. MacHugh. 2015. Analysis of the Bovine Monocyte-Derived Macrophage Response to Mycobacterium avium Subspecies Paratuberculosis Infection Using RNA-seq. *Front Immunol* 6: 23.
52. McLoughlin, K. E., N. C. Nalpas, K. Rue-Albrecht, J. A. Browne, D. A. Magee, K. E. Killick, S. D. Park, K. Hokamp, K. G. Meade, C. O'Farrelly, E. Gormley, S. V. Gordon, and D. E. MacHugh. 2014. RNA-seq Transcriptional Profiling of Peripheral Blood Leukocytes from Cattle Infected with Mycobacterium bovis. *Front Immunol* 5: 396.
53. He, Q., C. Zhang, L. Wang, P. Zhang, D. Ma, J. Lv, and F. Liu. 2015. Inflammatory signaling regulates hematopoietic stem and progenitor cell emergence in vertebrates. *Blood* 125: 1098-1106.
54. De Luca, K., V. Frances-Duvert, M. J. Asensio, R. Ihsani, E. Debien, M. Taillardet, E. Verhoeyen, C. Bella, S. Lantheaume, L. Genestier, and T. Defrance. 2009. The TLR1/2 agonist PAM(3)CSK(4) instructs commitment of human hematopoietic stem cells to a myeloid cell fate. *Leukemia* 23: 2063-2074.
55. Herman, A. C., D. A. Monlish, M. P. Romine, S. T. Bhatt, S. Zippel, and L. G. Schuettpelz. 2016. Systemic TLR2 agonist exposure regulates hematopoietic stem cells via cell-autonomous and cell-non-autonomous mechanisms. *Blood Cancer Journal* 6: e437.
56. Ziegler, G., D. Freyer, D. Harhausen, U. Khojasteh, W. Nietfeld, and G. Trendelenburg. 2011. Blocking TLR2 in vivo protects against accumulation of inflammatory cells and neuronal injury in experimental stroke. *J Cereb Blood Flow Metab* 31: 757-766.
57. Hoffmann, O., J. S. Braun, D. Becker, A. Halle, D. Freyer, E. Dagand, S. Lehnardt, and J. R. Weber. 2007. TLR2 mediates neuroinflammation and neuronal damage. *J Immunol* 178: 6476-6481.
58. Gu, Y., Y. Zhang, Y. Bi, J. Liu, B. Tan, M. Gong, T. Li, and J. Chen. 2015. Mesenchymal stem cells suppress neuronal apoptosis and decrease IL-10 release via the TLR2/NFkappaB pathway in rats with hypoxic-ischemic brain damage. *Mol Brain* 8: 65.
59. Kim, C., E. Rockenstein, B. Spencer, H. K. Kim, A. Adame, M. Trejo, K. Stafa, H. J. Lee, S. J. Lee, and E. Masliah. 2015. Antagonizing Neuronal Toll-like Receptor 2 Prevents Synucleinopathy by Activating Autophagy. *Cell Rep* 13: 771-782.
60. Moriguchi, T., M. Hamada, N. Morito, T. Terunuma, K. Hasegawa, C. Zhang, T. Yokomizo, R. Esaki, E. Kuroda, K. Yoh, T. Kudo, M. Nagata, D. R. Greaves, J. D. Engel, M. Yamamoto, and S. Takahashi. 2006. MafB is essential for renal development and F4/80 expression in macrophages. *Mol Cell Biol* 26: 5715-5727.
61. Bauquet, A. T., H. Jin, A. M. Paterson, M. Mitsdoerffer, I. C. Ho, A. H. Sharpe, and V. K. Kuchroo. 2009. The costimulatory molecule ICOS regulates the expression of c-Maf and IL-21 in the development of follicular T helper cells and TH-17 cells. *Nat Immunol* 10: 167-175.
62. Cao, S., J. Liu, L. Song, and X. Ma. 2005. The protooncogene c-Maf is an essential transcription factor for IL-10 gene expression in macrophages. *J Immunol* 174: 3484-3492.
63. Aziz, A., E. Soucie, S. Sarrazin, and M. H. Sieweke. 2009. MafB/c-Maf deficiency enables self-renewal of differentiated functional macrophages. *Science* 326: 867-871.
64. Richardson, E. T., S. Shukla, D. R. Sweet, P. A. Wearsch, P. N. Tsichlis, W. H. Boom, and C. V. Harding. 2015. Toll-like receptor 2-dependent extracellular signal-regulated kinase signaling in Mycobacterium tuberculosis-infected macrophages drives anti-inflammatory responses and inhibits Th1 polarization of responding T cells. *Infect Immun* 83: 2242-2254.
65. Piermattei, A., G. Migliara, G. Di Sante, M. Foti, S. B. Hayrabedyan, A. Papagna, M. C. Geloso, M. Corbi, M. Valentini, A. Sgambato, G. Delogu, G. Constantin, and F. Ria. 2016. Toll-Like Receptor 2 Mediates In Vivo Pro- and Anti-inflammatory Effects of Mycobacterium Tuberculosis and Modulates Autoimmune Encephalomyelitis. *Front Immunol* 7: 191.
66. Davila, S., M. L. Hibberd, R. Hari Dass, H. E. Wong, E. Sahiratmadja, C. Bonnard, B. Alisjahbana, J. S. Szeszko, Y. Balabanova, F. Drobniewski, R. van Crevel, E. van de Vosse, S. Nejentsev, T. H. Ottenhoff, and M. Seielstad. 2008. Genetic association and expression studies indicate a role of toll-like receptor 8 in pulmonary tuberculosis. *PLoS Genet* 4: e1000218.
67. Lai, Y. F., T. M. Lin, C. H. Wang, P. Y. Su, J. T. Wu, M. C. Lin, and H. L. Eng. 2016. Functional polymorphisms of the TLR7 and TLR8 genes contribute to Mycobacterium tuberculosis infection. *Tuberculosis (Edinb)* 98: 125-131.
68. Reeme, A. E., and R. T. Robinson. 2016. Dietary Vitamin D3 Suppresses Pulmonary Immunopathology Associated with Late-Stage Tuberculosis in C3HeB/FeJ Mice. *J Immunol* 196: 1293-1304.
69. Liu, P. T., S. Stenger, H. Li, L. Wenzel, B. H. Tan, S. R. Krutzik, M. T. Ochoa, J. Schauber, K. Wu, C. Meinken, D. L. Kamen, M. Wagner, R. Bals, A. Steinmeyer, U. Zugel, R. L. Gallo, D. Eisenberg, M. Hewison, B. W. Hollis, J. S. Adams, B. R. Bloom, and R. L. Modlin. 2006. Toll-like receptor triggering of a vitamin D-mediated human antimicrobial response. *Science* 311: 1770-1773.

70. Haire, R. N., J. P. Cannon, M. L. O'Driscoll, D. A. Ostrov, M. G. Mueller, P. M. Turner, R. T. Litman, G. W. Litman, and J. A. Yoder. 2012. Genomic and functional characterization of the diverse immunoglobulin domain-containing protein (DICP) family. *Genomics* 99: 282-291.
71. Rodriguez-Nunez, I., D. J. Wcisel, G. W. Litman, and J. A. Yoder. 2014. Multigene families of immunoglobulin domain-containing innate immune receptors in zebrafish: deciphering the differences. *Dev Comp Immunol* 46: 24-34.
72. Blander, J. M., and R. Medzhitov. 2004. Regulation of Phagosome Maturation by Signals from Toll-Like Receptors. *Science* 304: 1014-1018.
73. Rahman, M. J., O. D. Chuquimia, D. H. Petursdottir, N. Periolo, M. Singh, and C. Fernandez. 2011. Impact of toll-like receptor 2 deficiency on immune responses to mycobacterial antigens. *Infect Immun* 79: 4649-4656.
74. Li, M., R. Sun, L. Xu, W. Yin, Y. Chen, X. Zheng, Z. Lian, H. Wei, and Z. Tian. 2015. Kupffer Cells Support Hepatitis B Virus-Mediated CD8+ T Cell Exhaustion via Hepatitis B Core Antigen-TLR2 Interactions in Mice. *J Immunol* 195: 3100-3109.
75. van der Sar, A. M., H. P. Spaink, A. Zakrzewska, W. Bitter, and A. H. Meijer. 2009. Specificity of the zebrafish host transcriptome response to acute and chronic mycobacterial infection and the role of innate and adaptive immune components. *Mol Immunol* 46: 2317-2332.
76. Benard, E. L., A. M. van der Sar, F. Ellett, G. J. Lieschke, H. P. Spaink, and A. H. Meijer. 2012. Infection of zebrafish embryos with intracellular bacterial pathogens. *Journal of visualized experiments : JoVE*: 2.
77. Stockhammer, O. W., A. Zakrzewska, Z. Hegedus, H. P. Spaink, and A. H. Meijer. 2009. Transcriptome profiling and functional analyses of the zebrafish embryonic innate immune response to Salmonella infection. *J Immunol* 182: 5641-5653.
78. Loynes, C. A., J. S. Martin, A. Robertson, D. M. Trushell, P. W. Ingham, M. K. Whyte, and S. A. Renshaw. 2010. Pivotal Advance: Pharmacological manipulation of inflammation resolution during spontaneously resolving tissue neutrophilia in the zebrafish. *J Leukoc Biol* 87: 203-212.
79. Stoop, E. J. M., T. Schipper, S. K. Rosendahl Huber, A. E. Nezhinsky, F. J. Verbeek, S. S. Gurcha, G. S. Besra, C. M. J. E. Vandenbroucke-Grauls, W. Bitter, and A. M. van der Sar. 2011. Zebrafish embryo screen for mycobacterial genes involved in the initiation of granuloma formation reveals a newly identified ESX-1 component. *Dis Model Mech* 4: 526-536.
80. Ghotra, V. P., S. He, H. de Bont, W. van der Ent, H. P. Spaink, B. van de Water, B. E. Snaar-Jagalska, and E. H. Danen. 2012. Automated whole animal bio-imaging assay for human cancer dissemination. *PLoS One* 7: e31281.
81. van Soest, J. J., O. W. Stockhammer, A. Ordas, G. V. Bloemberg, H. P. Spaink, and A. H. Meijer. 2011. Comparison of static immersion and intravenous injection systems for exposure of zebrafish embryos to the natural pathogen Edwardsiella tarda. *BMC Immunol* 12: 58.
82. Livak, K. J., and T. D. Schmittgen. 2001. Analysis of relative gene expression data using real-time quantitative PCR and the 2(-Delta Delta C(T)) Method. *Methods* 25: 402-408.
83. Marin-Juez, R., S. Jong-Raadsen, S. Yang, and H. P. Spaink. 2014. Hyperinsulinemia induces insulin resistance and immune suppression via Ptpn6/Shp1 in zebrafish. *The Journal of endocrinology*.
84. Veneman, W. J., J. de Sonneville, K. J. van der Kolk, A. Ordas, Z. Al-Ars, A. H. Meijer, and H. P. Spaink. 2014. Analysis of RNAseq datasets from a comparative infectious disease zebrafish model using GeneTiles bioinformatics. *Immunogenetics*.
85. Veneman, W. J., J. de Sonneville, K. J. van der Kolk, A. Ordas, Z. Al-Ars, A. H. Meijer, and H. P. Spaink. 2015. Analysis of RNAseq datasets from a comparative infectious disease zebrafish model using GeneTiles bioinformatics. *Immunogenetics* 67: 135-147.
86. Love, M. I., W. Huber, and S. Anders. 2014. Moderated estimation of fold change and dispersion for RNA-seq data with DESeq2. *Genome Biol* 15: 550.
87. Kotelnikova, E., M. A. Shkrob, M. A. Pyatnitskiy, A. Ferlini, and N. Daraselia. 2012. Novel approach to meta-analysis of microarray datasets reveals muscle remodeling-related drug targets and biomarkers in Duchenne muscular dystrophy. *PLoS Comput Biol* 8: e1002365.

3